SUPPORTING INFORMATION

Robust covalent organic frameworks with tailor-made chelating sites for synergistic capture of U(VI) ions from highly acidic radioactive waste

Jipan Yu,[†a] Jianhui Lan,[†a] Shuai Wang,[a] Pengcheng Zhang,[a] Kang Liu,[a]

Liyong Yuan[*a], Zhifang Chai,[a,b] and Weiqun Shi[*a]

[a]Laboratory of Nuclear Energy Chemistry, Institute of High Energy Physics, Chinese Academy of Sciences, Beijing 100049, China

[b]Engineering Laboratory of Advanced Energy Materials, Ningbo Institute of Industrial Technology, Chinese Academy of Sciences, Ningbo, 315201, China

E-mail: yuanly@ihep.ac.cn; shiwq@ihep.ac.cn

[†]These authors contributed equally to this work

Table of Contents

Supplementary Text

General procedure for synthesis of compound TBBP, TBTA and DMPA

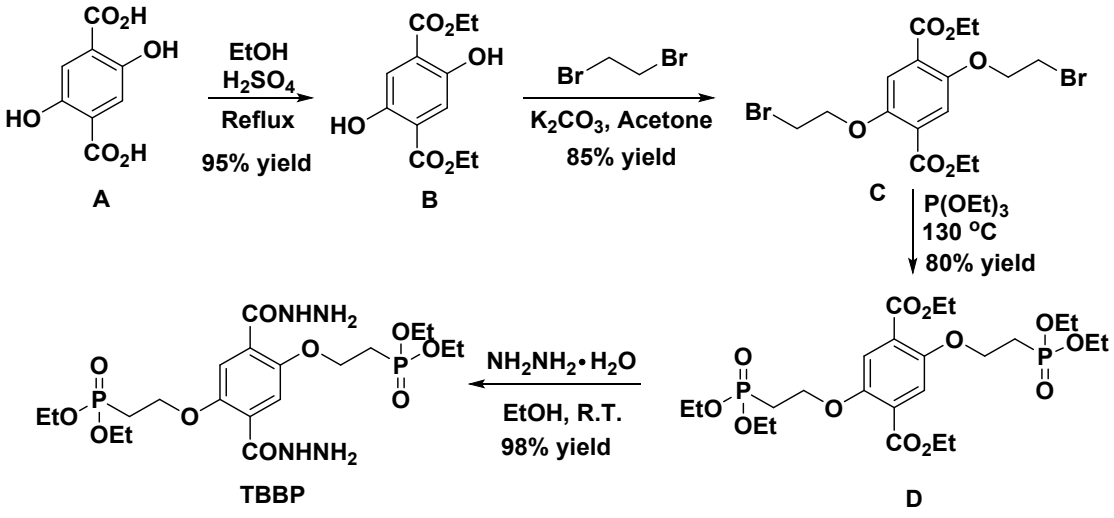

Scheme S1. Synthesis of TBBP

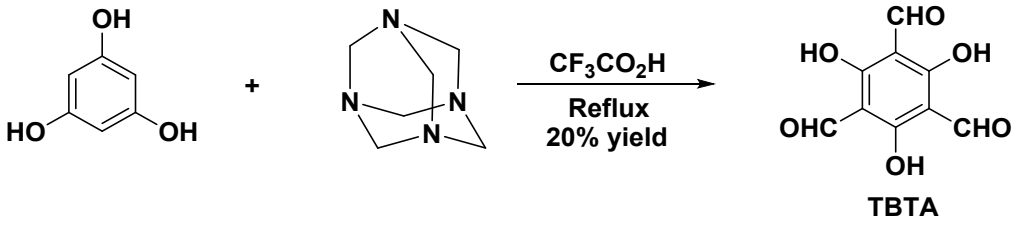

Scheme S2. Synthesis of TBTA

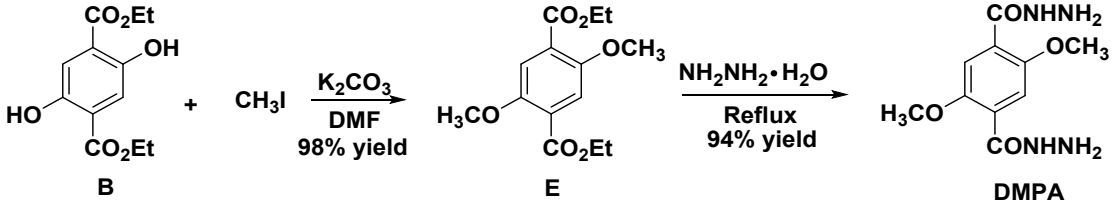

Scheme S3. Synthesis of DMPA

Synthesis of diethyl 2,5-dihydroxyterephthalate (**B**). Into a 100 ml round bottom flask were placed 5.0 g (25.2 mmol) of 2,5-dihydroxyterephthalate acid (**A**), 50 ml of ethanol and 8.0 ml of concentrated sulfuric acid. The mixture was refluxed for 8 h. After cooling to room temperature, abundant needle crystals precipitated and were

collected by filtration. After recrystallization from ethanol, 6.1 g of yellow green crystals **B** were obtained with a yield of 95%. ^{1}H NMR (500 MHz, $CDCl_3$): δ = 10.1 (s, 2H), 7.48 (s, 2H), 4.42 (q, J = 7.3 Hz, 4H), 1.43 (t, J = 7.3 Hz, 6H); ^{13}C NMR (125 MHz, $CDCl_3$): δ = 169.1, 152.9, 118.5, 117.7, 62.1, 14.1.

Synthesis of diethyl 2,5-bis(2-bromoethoxy)terephthalate (**C**). 2.54 g (10.0 mmol) of diethyl 2,5-dihydroxyterephthalate (**B**) were dissolved in 60 mL of acetone, to which 9.0 g of potassium carbonate was added. To the mixture, 8.6 mL (0.1 mol) of 1,2-dibromoethane was additionally added and heated to reflux for 24 h. After cooling to room temperature, the mixture was filtered and the filtrate was then evaporated to obtain the crude product, which was purified by flash chromatographic column (petroleum ether/ethyl acetate: 1/1) to afford **C** (3.96 g, 85% yield). ^{1}H NMR (500 MHz, $CDCl_3$): δ = 7.37 (s, 2H), 4.40-4.31 (m, 8H), 3.64 (t, J = 6.3 Hz, 4H), 1.39 (t, J = 6.3 Hz, 6H); ^{13}C NMR (125 MHz, $CDCl_3$): δ = 165.4, 151.6, 125.7, 118.1, 70.3, 61.7, 28.9, 14.4.

Synthesis of diethyl 2,5-bis(2-(diethoxyphosphoryl)ethoxy)terephthalate (**D**). 2.32 g (5.0 mmol) of diethyl 2,5-bis(2-bromoethoxy)terephthalate (**C**) and triethyl phosphite (8.3 g, 8.6 mL) were added to a 100 mL round bottom flask. The mixture was stirred at 130 ^{o}C for 36 h under nitrogen atmosphere. The resulting mixture was cooled to room temperature, the excess triethyl phosphite was removed by a rotary evaporator, and the residue was purified by flash chromatographic column (petroleum ether/ethyl acetate: 1/1) to afford **D** (2.33 g, 80% yield). ^{1}H NMR (500 MHz, $CDCl_3$): δ = 7.38 (s, 2H), 4.37 (q, J = 7.1 Hz, 4H), 4.27 (q, J = 8.4 Hz, 4H), 4.19-4.09 (m, 8H), 2.36 (dt, J = 18.9 Hz, J = 8.0 Hz, 4H), 1.42-1.32 (m, 18H); ^{13}C NMR (125 MHz, $CDCl_3$): δ = 165.4, 151.5, 125.4, 117.6, 64.6, 61.0 (d, $^{2}J_{C,P}$ = 6.3 Hz, $P(OCH_2CH_3)_2$), 61.5, 26.8 (d, $^{1}J_{C,P}$ = 140.2 Hz, $CP(OCH_2CH_3)_2$), 18.5 (d, $^{3}J_{C,P}$ = 6.0 Hz, $P(OCH_2CH_3)_2$), 14.4; ^{31}P NMR (151 MHz, $CDCl_3$): δ = 27.53;

Synthesis of diethyl 2,5-bis(2-(diethoxyphosphoryl)ethoxy)terephthalate (**TBBP**). 1.16 g (2.0 mmol) of diethyl 2,5-bis(2-(diethoxyphosphoryl)ethoxy)terephthalate (**D**) was dissolved in 20 mL ethanol and 2 mL of hydrazine hydrate. The mixture was stirred at room temperature for 4 h. After the reaction was complete, the solvent was

evaporated to obtain the crude product as a light yellow solid, which was washed with petroleum ether. The light yellow solid was dried to almost quantitatively obtain the product. ^{1}H NMR (500 MHz, $CDCl_3$): δ = 9.88 (s, 2H), 7.82 (s, 2H), 4.42 (dt, J = 21.0 Hz, J = 6.0 Hz, 4H), 4.20-4.13 (m, 12H), 2.33 (dt, J = 17.8 Hz, J = 6.0 Hz, 4H), 1.33 (t, J = 7.1 Hz, 12H); ^{13}C NMR (125 MHz, $CDCl_3$): δ = 163.6, 150.1, 123.6, 115.2, 63.3 (d, $^{2}J_{C,P}$ = 6.6 Hz, OCH_2CH_2P), 62.3 (d, $^{2}J_{C,P}$ = 6.5 Hz, P(OCH_2CH_3)$_2$), 26.3 (d, $^{1}J_{C,P}$ = 144.0 Hz, CH_2P(OCH_2CH_3)$_2$), 16.5 (d, $^{3}J_{C,P}$ = 5.7 Hz, P(OCH$_2$$CH_3$)$_2$); ^{31}P NMR (151 MHz, $CDCl_3$): δ = 28.12;

Synthesis of 2,4,6-trihydroxybenzene-1,3,5-tricarbaldehyde (TBTA)[1]: 1,3,5-Triformylphloroglucinol has been synthesized using previously reported methods. To a mixture of 7.4 g hexamethylenetetramine and 3 g of phloroglucinol, trifluoroacetic acid (45 mL) was added at 0 ^{o}C. The mixture was then slowly increased to room temperature. The solution was then allowed to reflux at 100 °C for 2.5 h under nitrogen atmosphere. After that time period 3 M HCl was added to it slowly and was further refluxed for another 1h. Finally, the mixture was allowed to cool to room temperature and filtered through celite. The filtrate was extracted with CH_2Cl_2 (3 times) and dried over anhydrous Na_2SO_4. The obtained extract was concentrated to yield dull yellow colored solid. The pure product was obtained via recrystallization with hot ethanol, the yield is 20%. ^{1}H NMR (500 MHz, $CDCl_3$): δ = 10.02 (s, 3H), 7.94 (s, 3H); ^{13}C NMR (125 MHz, $CDCl_3$): δ = 191.9, 173.8, 103.6.

Synthesis of dimethyl 2,5-diethoxyterephthalate (E): Diethyl 2,5-dihydroxyterephthalate **B** (4.0 g, 15.7 mmol) and potassium carbonate (10.0 g, 72.3 mmol) were placed in a dry 150 mL round bottom flask equipped with a stir bar, which was then sealed with a septum, and purged with N_2. DMF (78.7 mL) and iodomethane (37.8 mmol) were subsequently added by syringe. The reaction mixture was heated to 90 °C for 8.5 h. Upon full conversion by thin layer chromatography (hexanes/EtOAc, 9:1), the reaction was quenched with aqueous HCl (1 M, 10 mL) and the resulting precipitate was isolated by filtration and dried under vacuum. The resulting dimethyl 2,5-diethoxyterephthalate (4.41 g, 98% yield) was isolated as a white solid that required no further purification.

Synthesis of 2,5-dimethoxyterephthalohydrazide (DMPA): Dimethyl 2,5-

diethoxyterephthalate (4.1 g, 14.5 mmol) was dissolved in EtOH (50 mL) in a 150 mL round bottom flask equipped with a stir bar. Hydrazine hydrate (8.5 mL, 174 mmol) was added and the flask was then equipped with a condenser and heated to reflux for 15 h. The reaction was then allowed to cool to rt, and a while precipitate formed. The flask was then placed in the freezer for 3.5 h. The white needles were isolated by filtration, washed three times with EtOH, and dried under vacuum. DMPA was isolated as white needles (3.46 g, 94%). ^{1}H NMR (500 MHz, DMSO-d_6): δ = 9.35 (s, 2H), 7.39 (s, 2H), 4.58 (s, 4H), 3.85 (s, 6H); ^{13}C NMR (125 MHz, DMSO-d_6): δ = 164.1, 150.8, 125.2, 113.9.

General procedure for Synthesis of COF-JLU4, COF-IHEP10 and COF-IHEP11

Synthesis of COF-JLU4[2]**:** A glass ampoule (volume of *ca.* 20 mL, body length of 18 cm) was charged with 2,4,6-trihydroxybenzene-1,3,5-tricarbaldehyde (TBTA, 21 mg, 0.10 mmol) and 2,5-dimethoxyterephthalohydrazide (DMPA, 38 mg, 0.15 mmol). To the mixture were added anhydrous 1,4-dioxane (1.0 mL) and mesitylene (3.0 mL). The tube was immersed in an ultrasonic bath for 15 min; following sonication 0.4 mL of 6 mol/L aqueous acetic acid was added and the Pyrex tube was degassed by three freeze-pump-thaw cycles. The tube was then sealed off and heated at 120 °C and left undisturbed for 72 h, yielding a pale-yellow solid at the bottom of the tube. The precipitate was isolated by filtration and washed with anhydrous THF (3 × 10 mL) and anhydrous acetone (3 × 10 mL); the resulting powder was dried at 80 ºC under 10^{-2} mTorr for 12 h to yield COF-JLU4 as a light yellow powder (46 mg, 87% yield). Elemental analysis for $(C_8H_7N_2O_3)_n$: C 53.63; H 3.91; N 15.64. Found (%): C 53.87; H 4.04; N 16.15.

Synthesis of COF-IHEP10: A glass ampoule (volume of *ca.* 20 mL, body length of 18 cm) was charged with 2,4,6-trihydroxybenzene-1,3,5-tricarbaldehyde (TBTA, 21 mg, 0.10 mmol) and 2,5-dimethoxyterephthalohydrazide (DMPA, 19 mg, 0.075 mmol) and tetraethyl ((2,5-di(hydrazinecarbonyl)-1,4-phenylene)bis(oxy))bis(ethane-2,1-diyl))bis (phosphonate) (TBBP, 41.5 mg, 0.075 mmol). To the mixture were added anhydrous 1,4-dioxane (1.0 mL) and mesitylene (3.0 mL). The tube was immersed in

an ultrasonic bath for 15 min; following sonication 0.4 mL of 6 mol/L aqueous acetic acid were added and the Pyrex tube was degassed by three freeze-pump-thaw cycles. The tube was then sealed off and heated at 120 °C and left undisturbed for 72 h, yielding a pale-yellow solid at the bottom of the tube. The precipitate was isolated by filtration and washed with anhydrous THF (5 × 10 mL) and anhydrous acetone (3 × 10 mL), the resulting powder was dried at 80 ºC under 10^{-2} mTorr for 12 h to yield COF-IHEP10 as a light yellow powder (67 mg, 88% yield). Elemental analysis for $(C_{21}H_{25}N_4O_9P_1)_n$: C 49.61; H 4.92; N 11.16; P 6.10. Found (%): C 48.62; H 5.51; N 10.09; P 5.89.

Synthesis of COF-IHEP11: A glass ampoule (volume of *ca.* 20 mL, body length of 18 cm) was charged with and 2,4,6-trihydroxybenzene-1,3,5-tricarbaldehyde (TBTA, 21 mg, 0.10 mmol) and tetraethyl (((2,5-di(hydrazinecarbonyl)-1,4-phenylene)bis(oxy))bis(ethane-2,1-diyl))bis(phosphonate) (TBBP, 83 mg, 0.15 mmol). To the mixture were added anhydrous 1,4-dioxane (1.0 mL) and mesitylene (3.0 mL). The tube was immersed in an ultrasonic bath for 15 min; following sonication, 0.4 mL of 6 mol/L aqueous acetic acid were added and the Pyrex tube was degassed by three freeze-pump-thaw cycles. The tube was then sealed off and heated at 120 °C and left undisturbed for 72 h, yielding a off-white solid at the bottom of the tube. The precipitate was isolated by filtration and washed with anhydrous THF (5 × 10 mL) and anhydrous acetone (3 × 10 mL), the resulting powder was dried at 80 ºC under 10^{-2} mTorr for 12 h to yield COF-IHEP11 as a light yellow powder (90 mg, 91% yield). Elemental analysis for $(C_{13}H_{18}N_2O_6P)_n$: C 48.00; H 5.54; N 7.38; P 9.54. Found (%): C 49.35; H 5.12; N 9.00; P 9.72.

Characterization

Proton and carbon magnetic resonance spectra (^{1}H NMR、^{13}C NMR and ^{31}P NMR) were recorded using tetramethylsilane (TMS) in solvent of $CDCl_3$ as the internal standards (^{1}H NMR: TMS at 0.00 ppm, $CDCl_3$ at 7.26 ppm; ^{13}C NMR: $CDCl_3$ at 77.26 ppm). A Bruker D8 Advance diffractometer (Cu Kα radiation, λ = 1.5406 Å) was used to collect powder X-ray diffraction (XRD) patterns. The step size for XRD pattern scanning was 0.02 Å. Bruker Tensor 27 spectrometer was used to record the

Fourier transform infrared (FTIR) spectra of samples by a potassium bromide pellet method. The residual concentrations of uranium and other metal S-3 elements were determined by an inductively coupled plasma optical emission spectrograph (ICP-OES, Horiba JY2000-2, Japan). Thermogravimetric curve was recorded on a thermal gravimetric analyzer (TGA, TA Instruments, Q500) from 20-800 ^{o}C by using a heating rate of 5 ^{o}C min^{-1} under air flow. The N_2 sorption experiments were measured at liquid nitrogen temperature (-196 ^{o}C) using a micromeritics ASAP 2020 HD88 instrument. The samples were pretreated at 120 ^{o}C for 8 h. S-3 The surface area was calculated by the Brunauer-Emmett-Teller (BET) method. The total pore volume was evaluated by the single point method. Solid-state NMR experiments were performed on a JEOL-800 MHz NMR spectrometer. The ^{13}C CP/MAS NMR spectra were recorded with a 4-mm double-resonance MAS probe and with a sample spinning rate of 10.0 kHz; a contact time of 2 ms (ramp 100) and a pulse delay of 3 s were applied.

Structural modeling and PXRD analysis of COF-IHEP10 and COF-IHEP11 as well as adsorption mechanism investigations

Crystal models of COF-IHEP10 and COF-IHEP11 were generated with the Crystal Building module of the Material Studio software. The initial lattices were firstly created by starting with COF-JLU4 obtained by Xiaoming Liu et al.[3] These materials possess similar topology frameworks with our COFs. The c cell parameter was kept with a distance of 3.60 Å for the bnn topology, similar as observed in other COFs especially COF-JLU4 and TpPa-1/2. We then performed a series of geometry optimizations with the UFF force field at the ultra-fine quality in the Forcite module, allowing optimizing all the lattice parameters and atomic coordinates. Different algorithms can direct to somewhat different conformations of COFs. However, the best conformation was obtained from comparison of simulated PXRD patterns with the experimental patterns. Based on the obtained results, subsequent simulation of powder diffraction patterns with the Reflex module in Materials studio was performed. Only the bnn topology was tried based on the fact that the simulated XRD pattern in terms of this mode generally fits better with the experimental one than the gra mode as reported in related literatures. During our building of the COFs, the space group was reduced to P6 and P1 for COF-IHEP11 and COF-IHEP10, respectively. Pawley

refinement was done with the Reflex module. The Pawley refinement was performed to iteratively optimize the lattice parameters until the R_{wp} value converges and the observed profile fits well with the refined one. For COF-IHEP10 and COF-IHEP11, we found that the PXRD from the bnn topology agrees well with the experimental data. That means that bnn is likely the dominant topology in the synthesized products.

To probe the adsorption mechanism of uranyl ions with COFs, we further explored density functional theory (DFT) calculations using the Vienna ab initio simulation package VASP 5.4.[4] The projector-augmented-wave (PAW) potentials[5] and a plane-wave basis set have been applied here. To describe the exchange correlation energy functional, the generalized gradient approximation (GGA) parameterized by Perdew, Burke, and Ernzerhof (PBE)[6] was adopted. For uranium, the U $6s^2 6p^6 5f^3 6d^1 7s^2$ valence electrons were treated explicitly. The plane-wave cutoff was set to be 400 eV. The geometries were optimized until the forces are smaller than 0.05 eV/Å. The total energy was relaxed until the difference value is smaller than 10^{-5} eV. The integrations in the reciprocal space were replaced by summation on the 1 × 1× 1 Monkhost-Pack grid.[7] A single layer of COF-IHEP11 was selected as the representative model with a interlayer spacing of 20 Å in all calculations.

Batch sorption experiments

A series of tests for the sorption of U(VI) from aqueous solutions onto COFs as a function of pH, contact time, initial U(VI) concentration and competing metal cations were performed. A 42 mmol L^{-1} U(VI) stock solution was first prepared by dissolving appropriate amounts of uranyl nitrate hexahydrate in Milli-Q water (18.2 MΩ cm^{-1}). U(VI) sorption experiments were performed by using a batch method with initial concentrations ranging from 5 to 120 mg L^{-1} at room temperature. Small quantities of 0.1 M HNO_3 and 0.1 M NaOH solutions were used to adjust the solution pH. In a typical experiment, 4 mg of sorbent was added into either 10 mL U(VI) solution or 10 ml multi-ion test solution in a flask (viz. the solid-liquid ratio was 0.4 mg mL^{-1}). The flasks were stirred for 6 h at room temperature, and then the sorbent was separated from the solution using a 0.22 μm nylon syringe filter (ANPEL Scientific Instrument Co., Ltd., Shanghai). Before determining the cationic concentrations, the initial

solution and the supernatants, before and after the sorption, were diluted 2.5~100 times to make sure that the U(VI) concentration in the dilution is 0.1~5 μg/mL. The concentrations of U(VI) in diluted solutions were determined by spectrophotometric method. All values were measured in duplicate; the uncertainties in the concentrations was within 5%. The sorption efficiency (*E*） and the sorption capacity (q_e) of U(VI)) were defined as follows:

$$E(\%) = \frac{C_0 - C_e}{C_0} \times 100\% \quad (1)$$

$$q_e = \frac{C_0 - C_e}{m_{sorbent}} \times V_{solution} \quad (2)$$

where c_0 and c_e are the initial concentration and equilibrium concentration of the metal cations (mg L^{-1}), respectively. *V* is the volume of the testing solution (mL), and *m* is the amount of sorbent (g).

Supplementary Figures

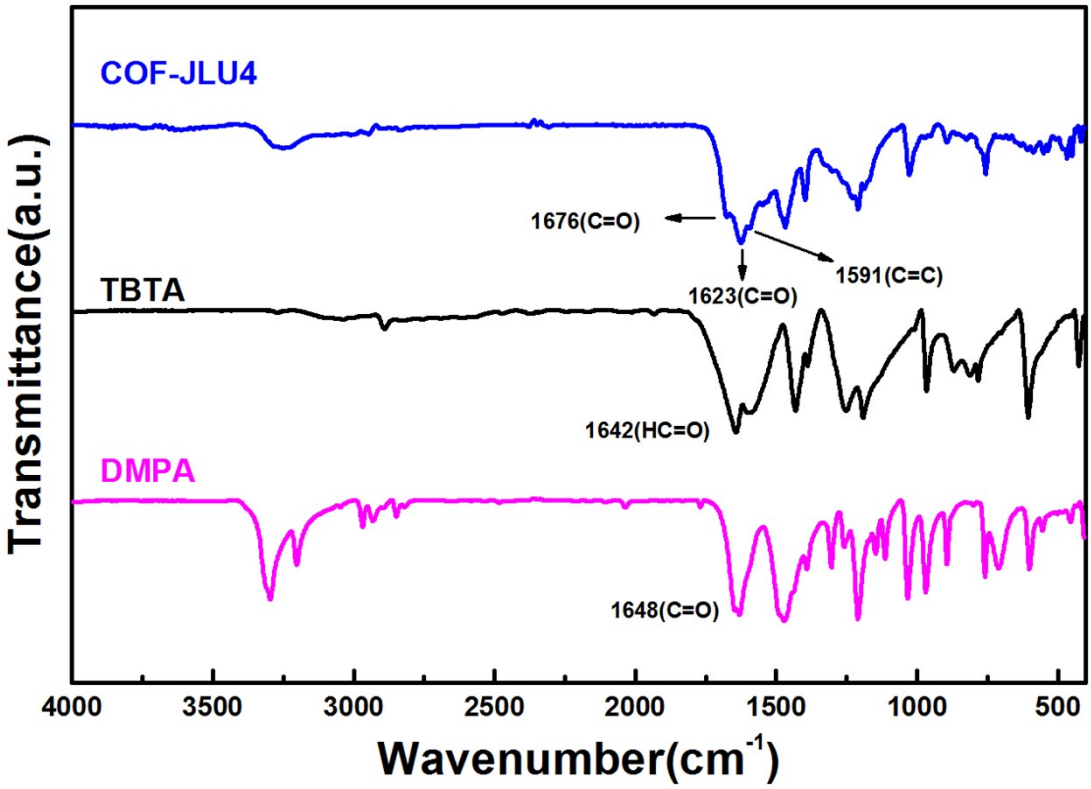

Figure S1. IR spectra of COF-JLU4 and corresponding monomers

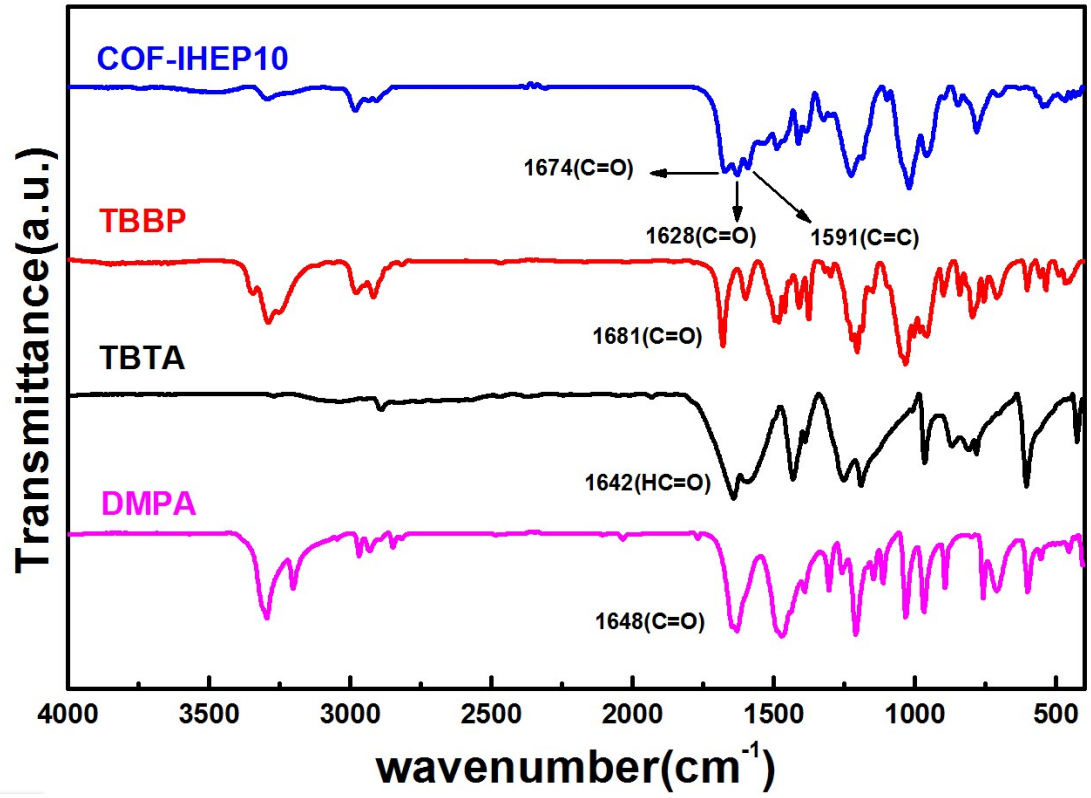

Figure S2. IR spectra of COF-IHEP10 and corresponding monomers

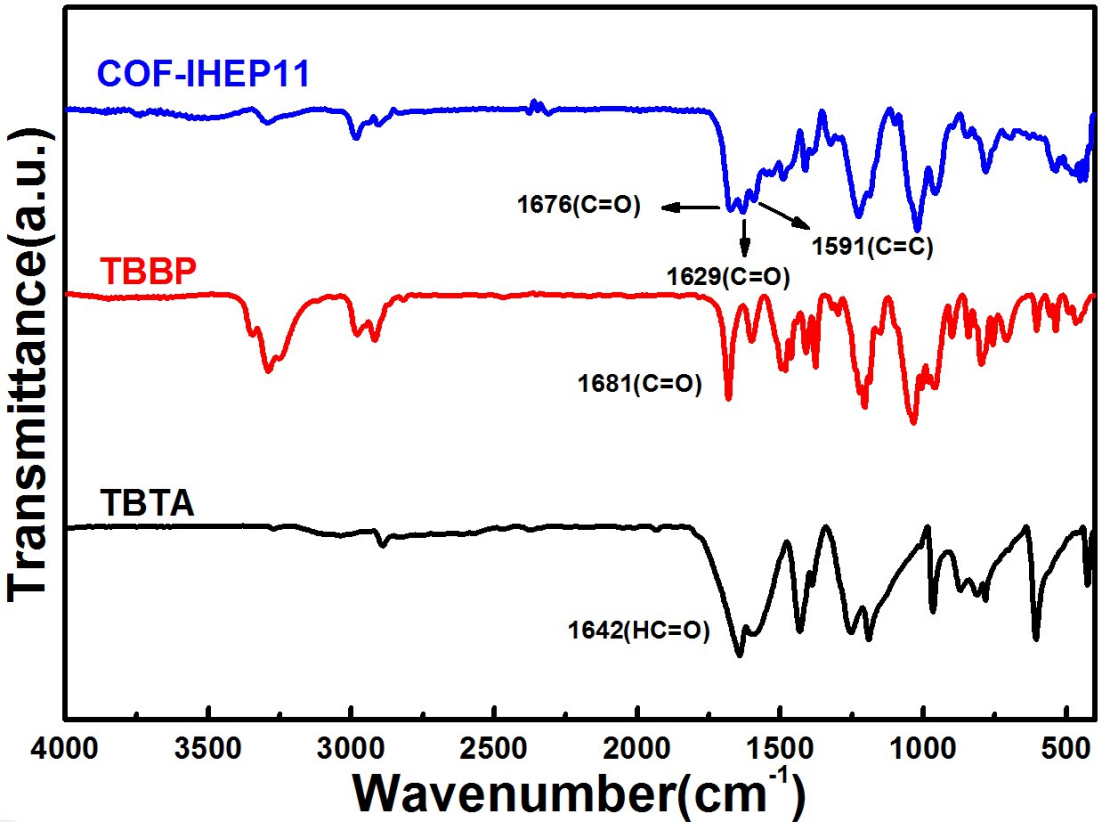

Figure S3. IR spectra of COF-IHEP11 and corresponding monomers

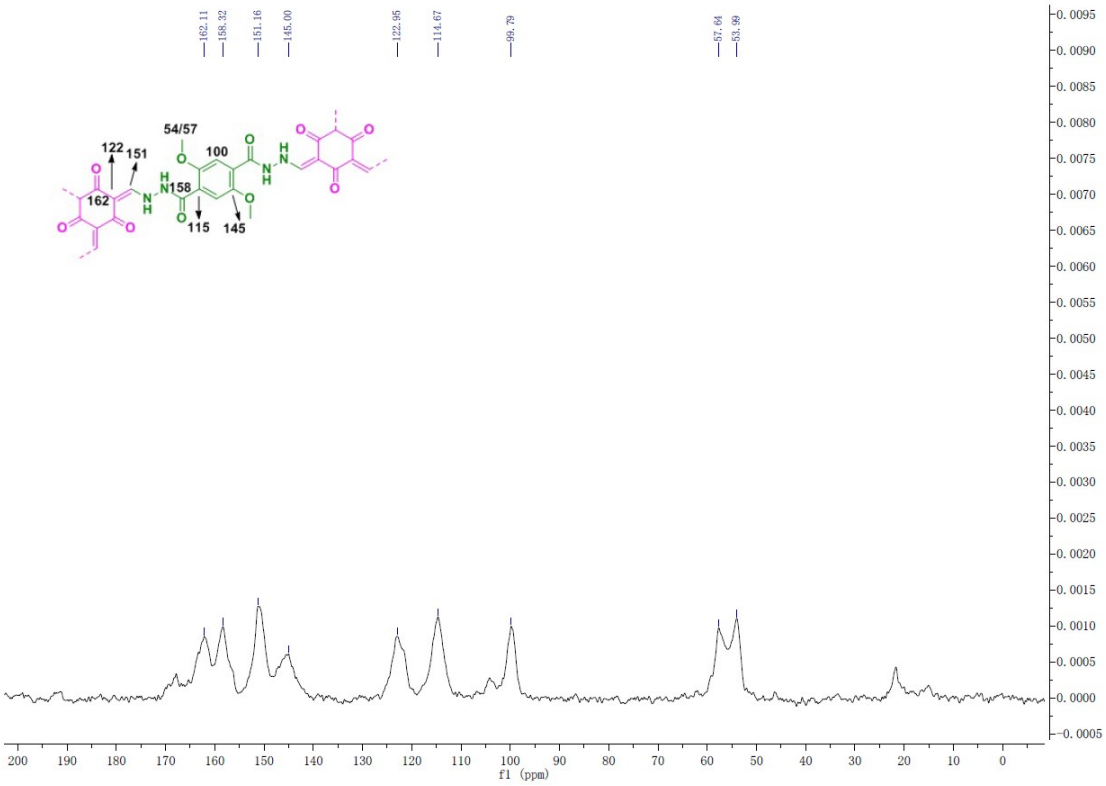

Figure S4. ^{13}C CP/MAS NMR spectra of COF-JLU4

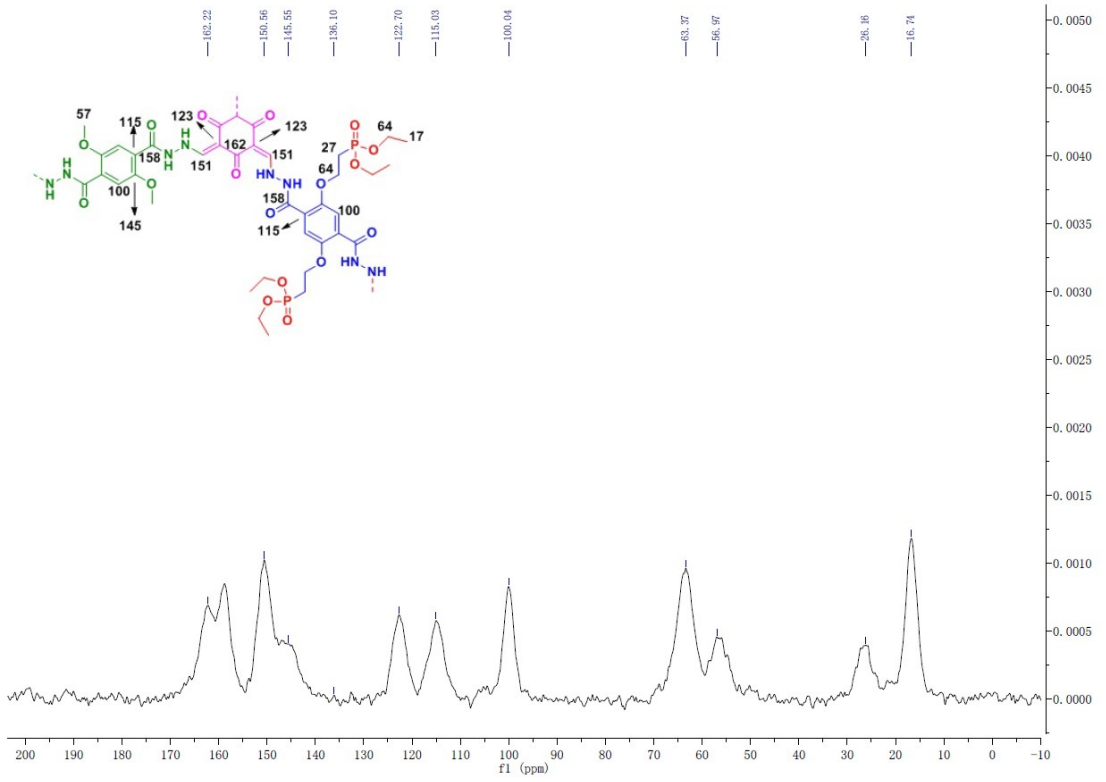

Figure S5. ^{13}C CP/MAS NMR spectra of COF-IHEP10

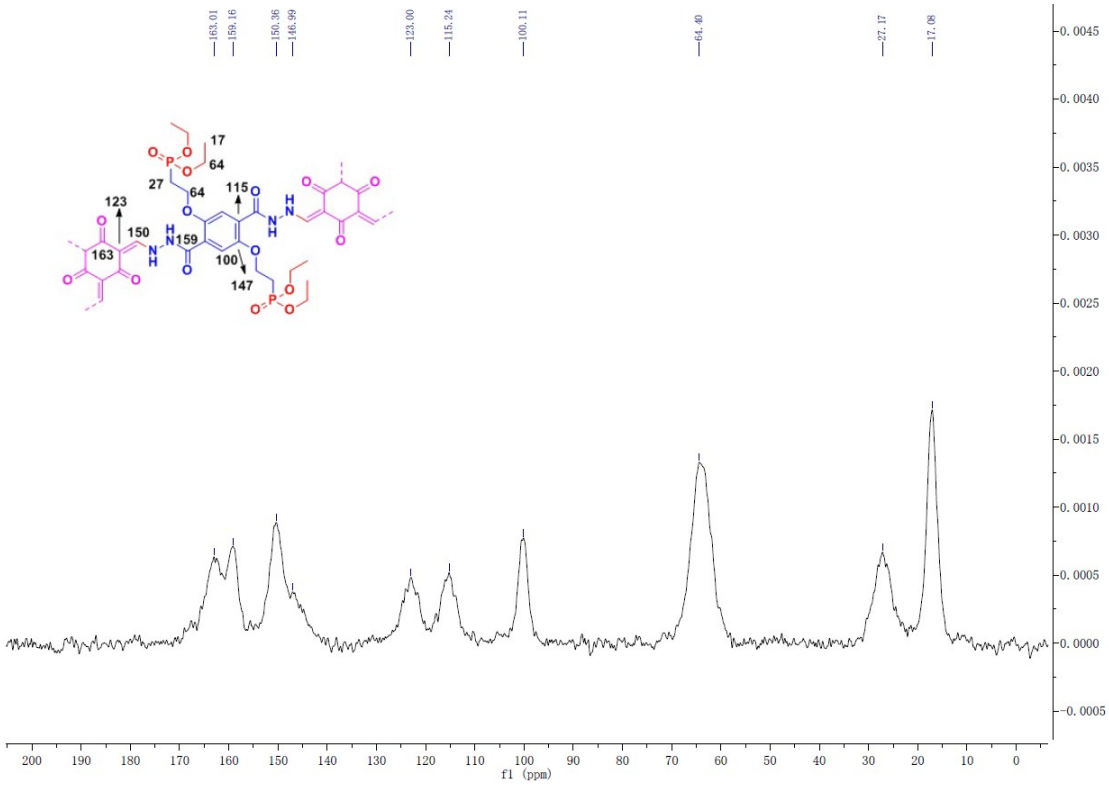

Figure S6. ^{13}C CP/MAS NMR spectra of COF-IHEP11

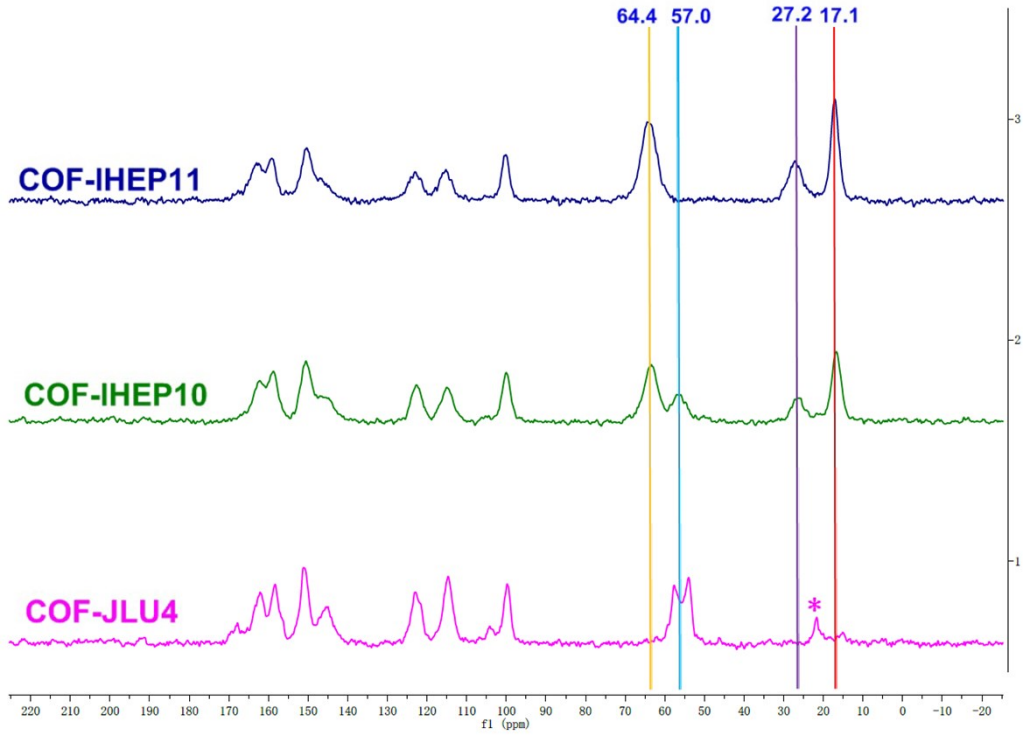

Figure S7. ^{13}C MAS NMR spectra of COF-JLU4, COF-IHEP10 and COF-IHEP11

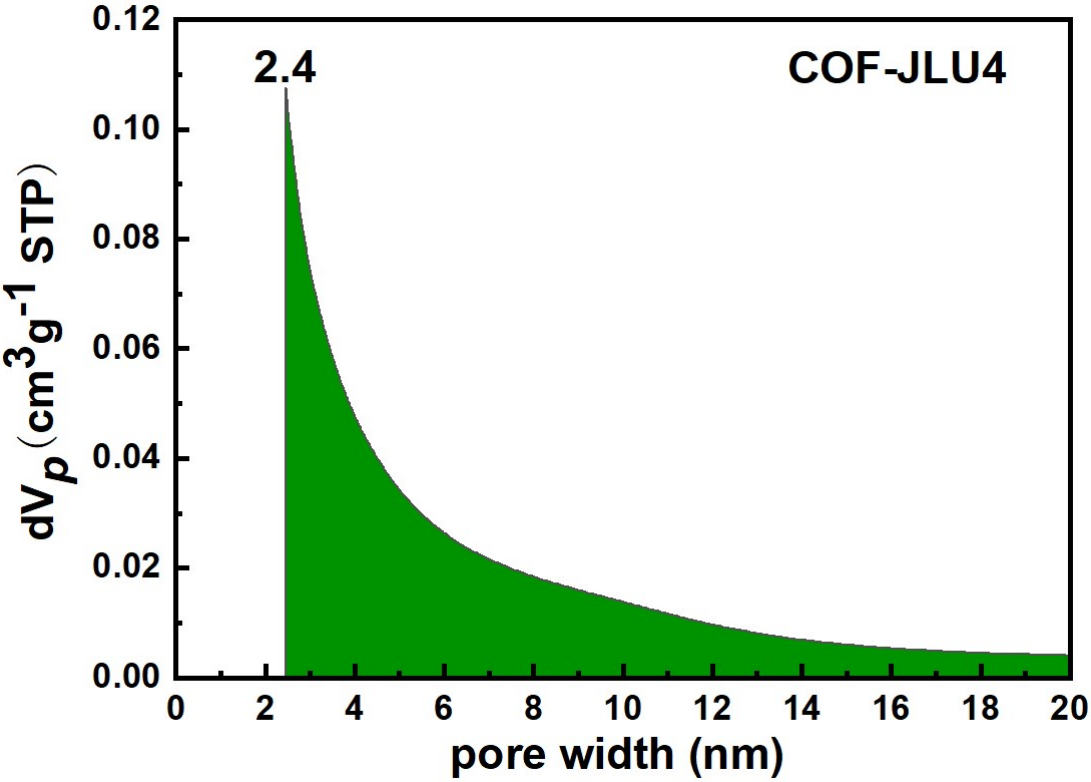

Figure S8. Pore With of COF-JLU4

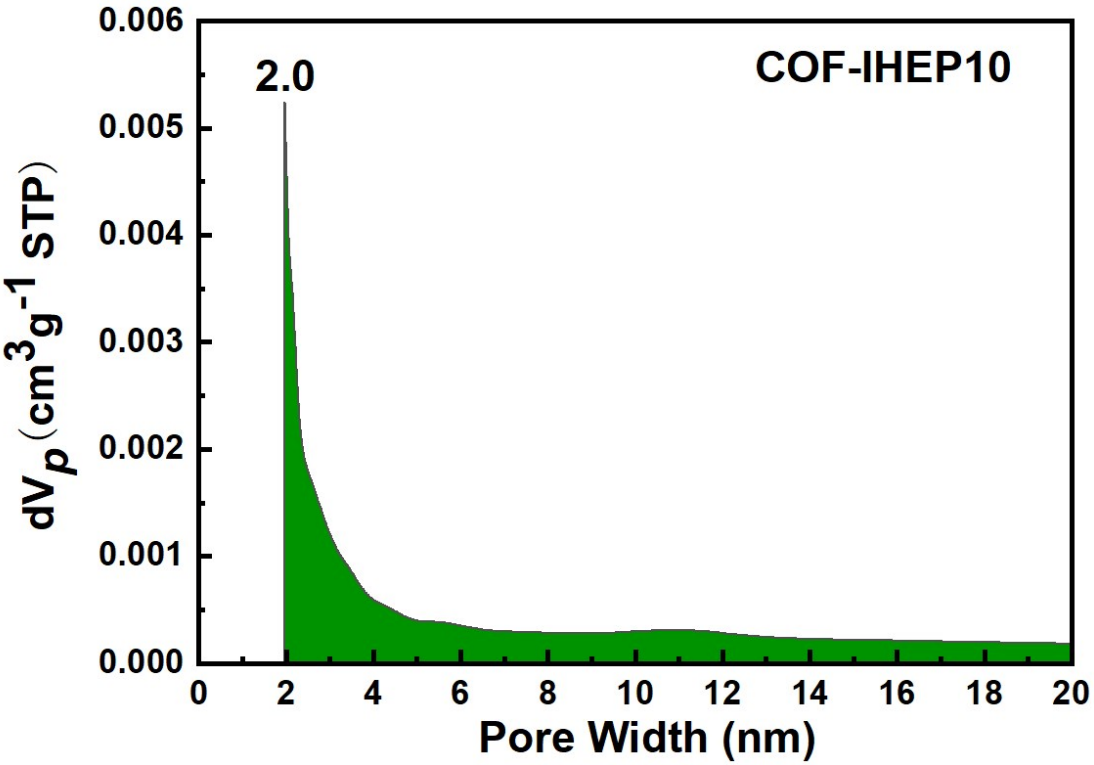

Figure S9. Pore With of COF-IHEP10

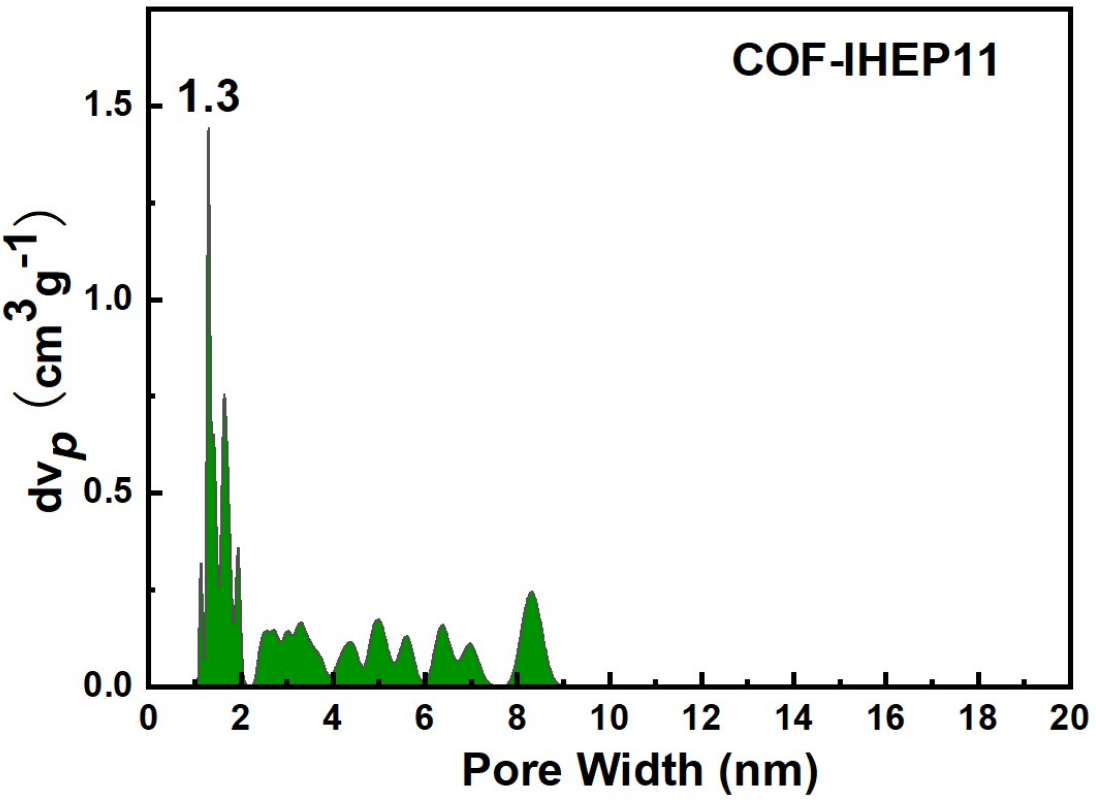

Figure S10. Pore With of COF-IHEP11

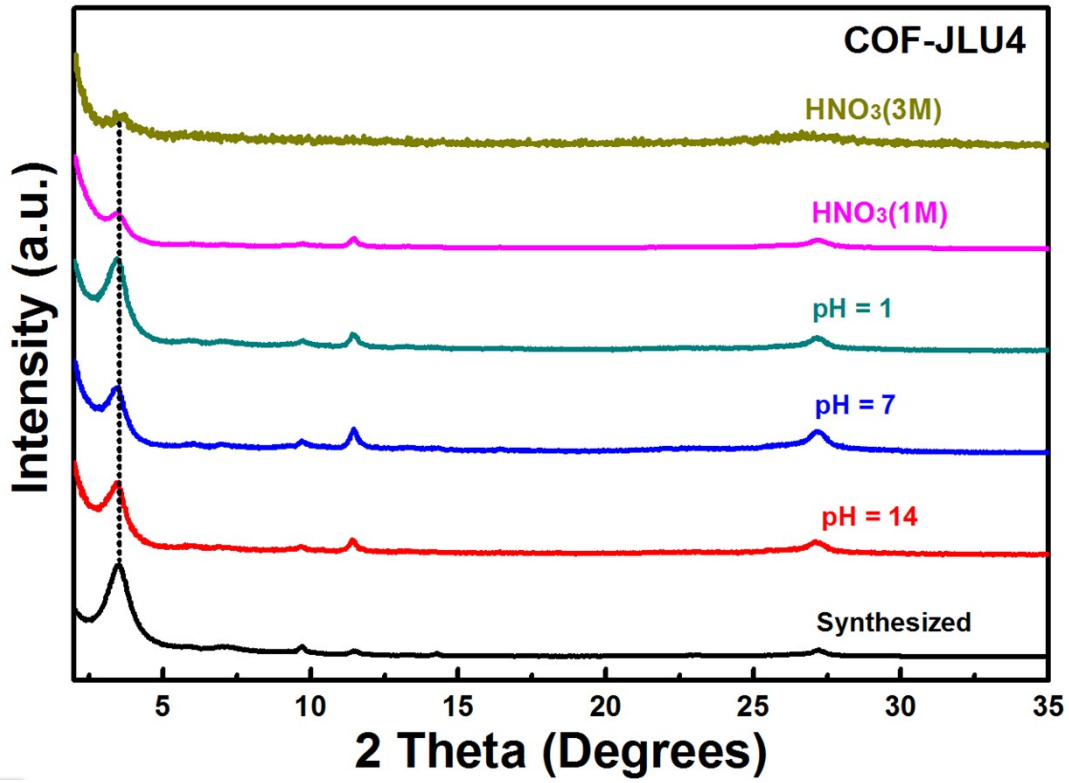

Figure S11. PXRD patterns of COF-JLU4 before and after the treatment in aqueous solutions with different acidic values

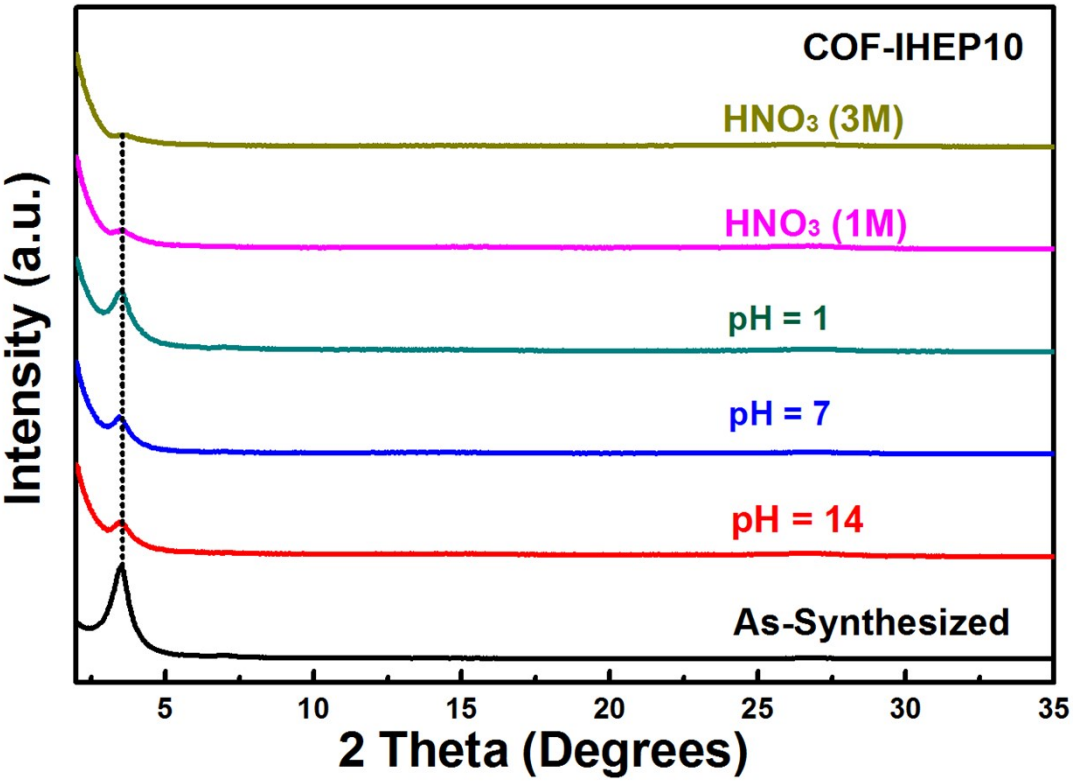

Figure S12. PXRD patterns of COF-IHEP10 before and after the treatment in aqueous solutions with different acidic values

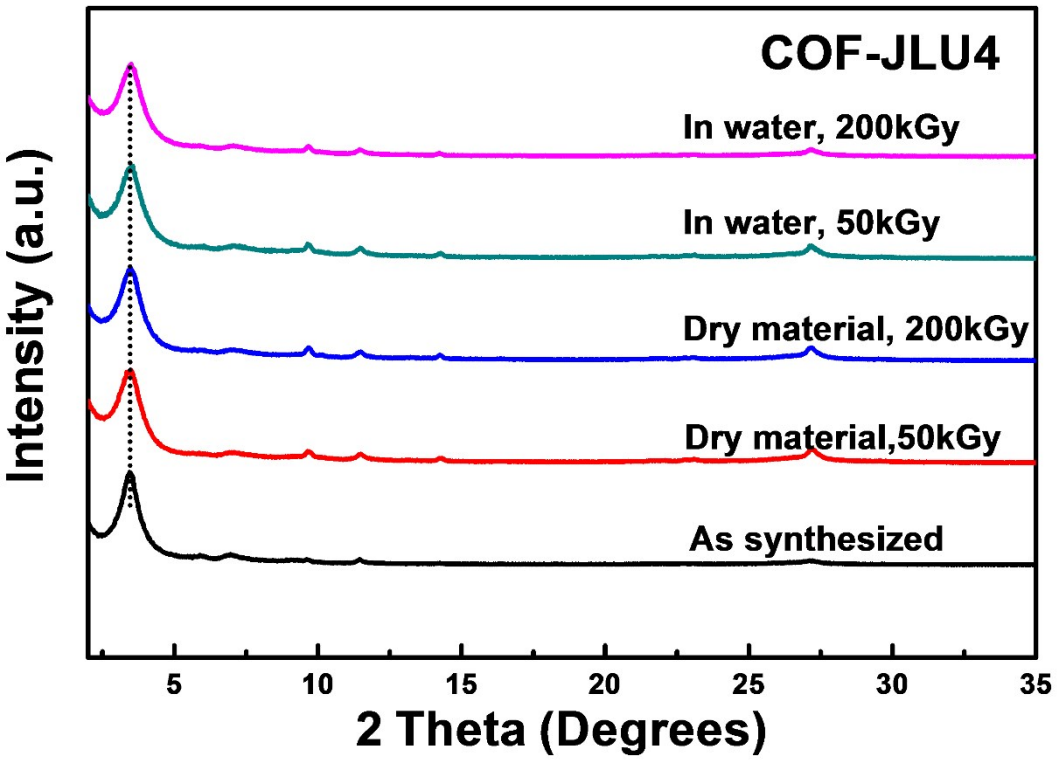

Figure S13. Stability of COF-JLU4 after Gamma Irradiation

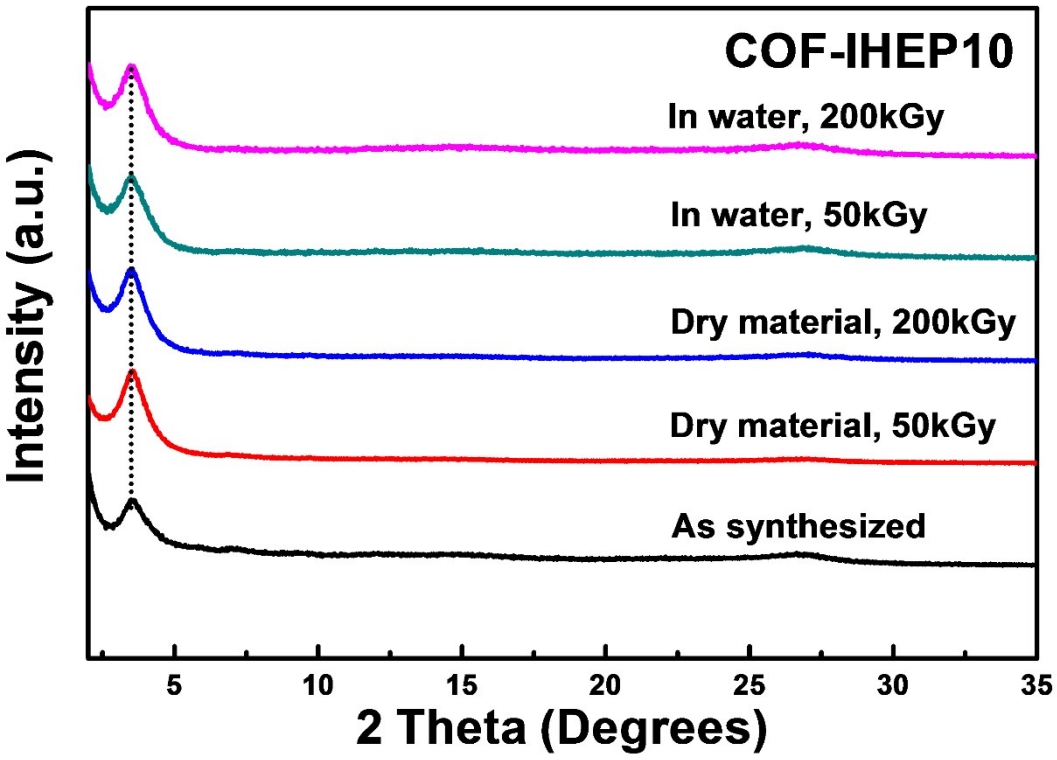

Figure S14. Stability of COF-IHEP10 after Gamma Irradiation

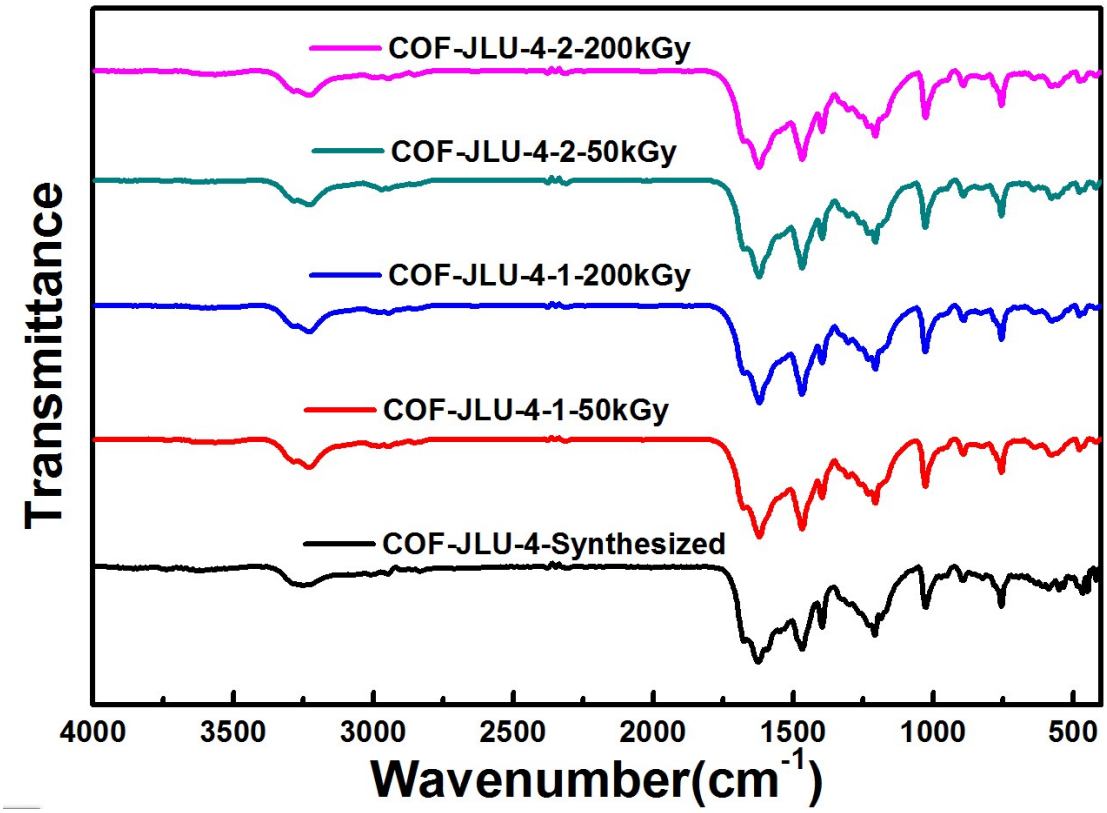

Figure S15. FT-IR of COF-JLU4 after Gamma Irradiation

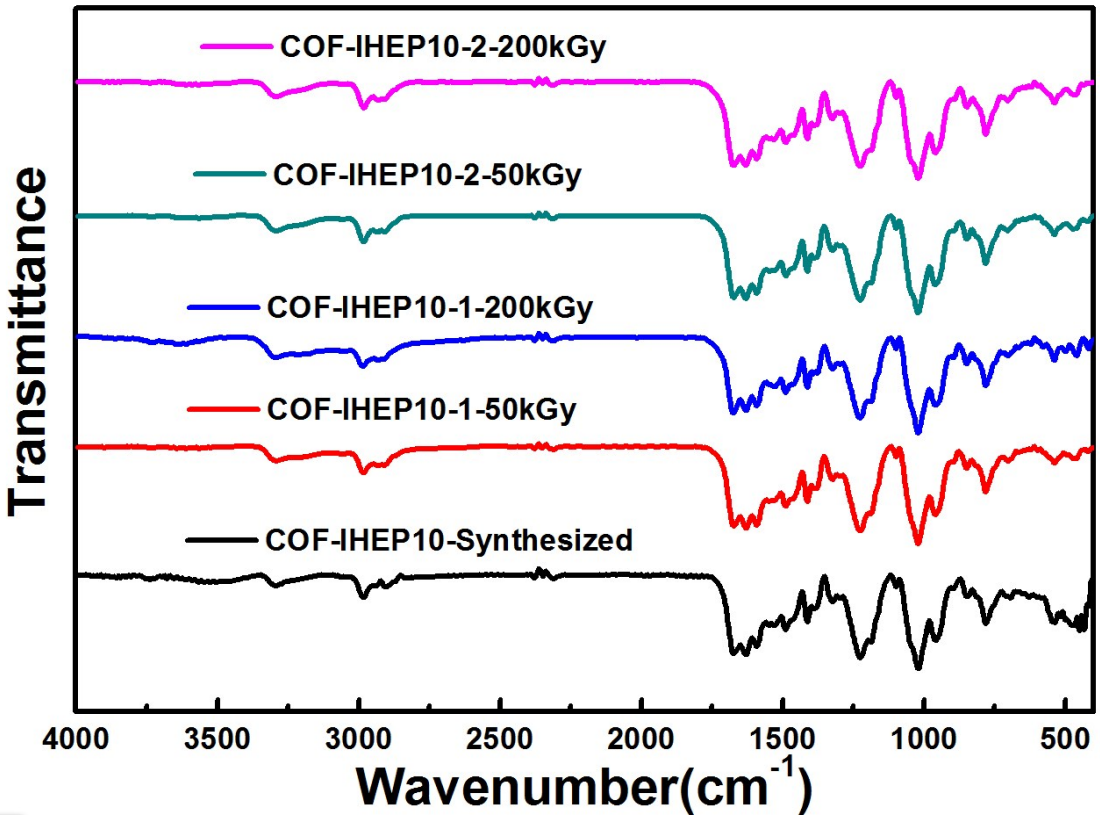

Figure S16. FT-IR of COF-IHEP10 after Gamma Irradiation

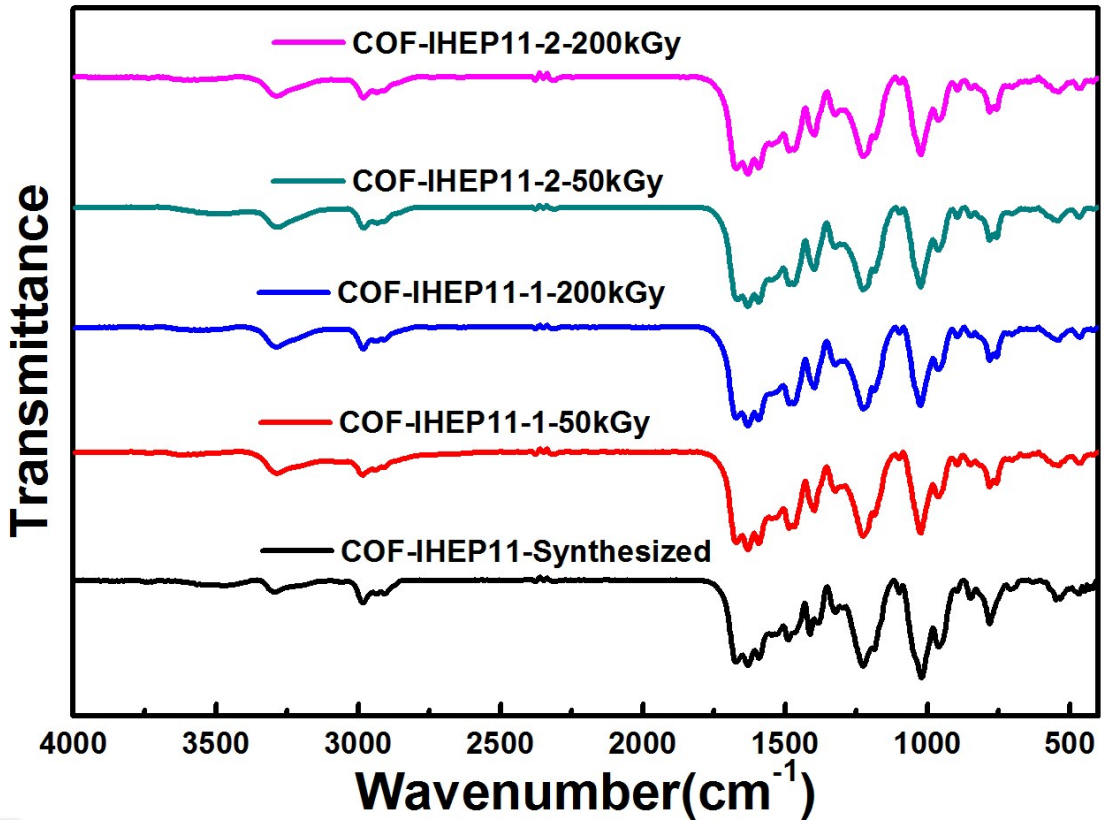

Figure S17. FT-IR of COF-IHEP11 after Gamma Irradiation

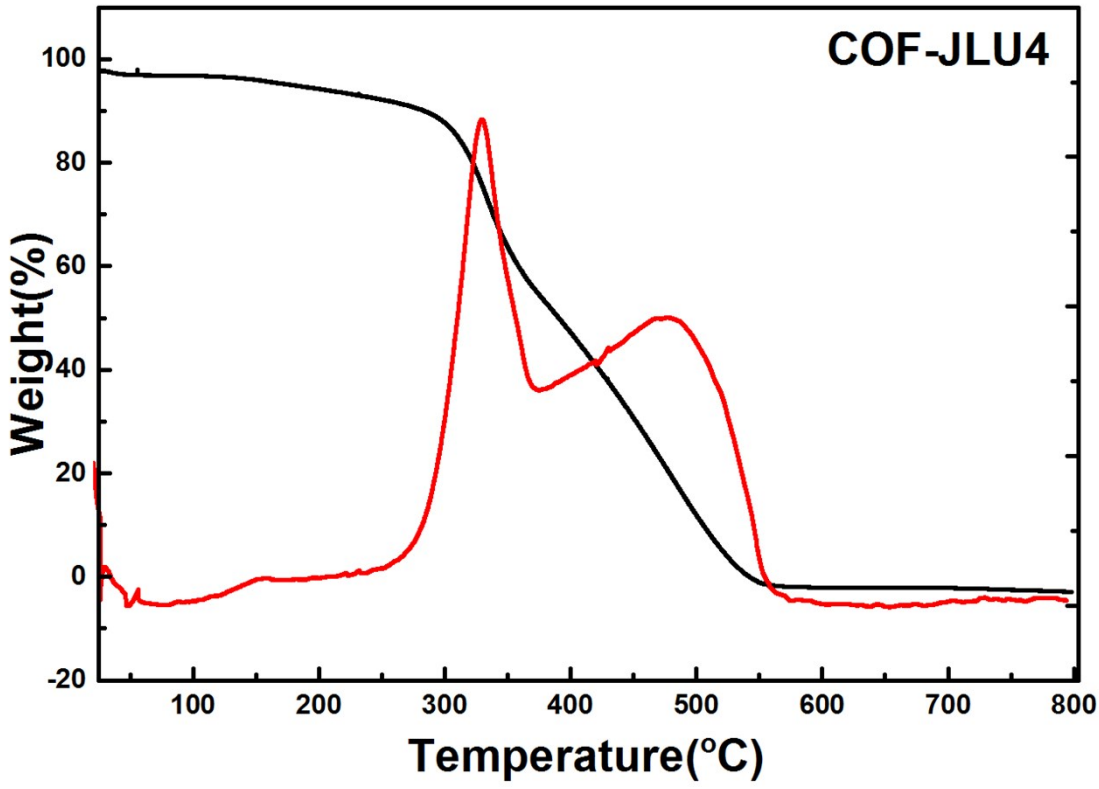

Figure S18. Thermogravimetric Analysis of COF-JLU4

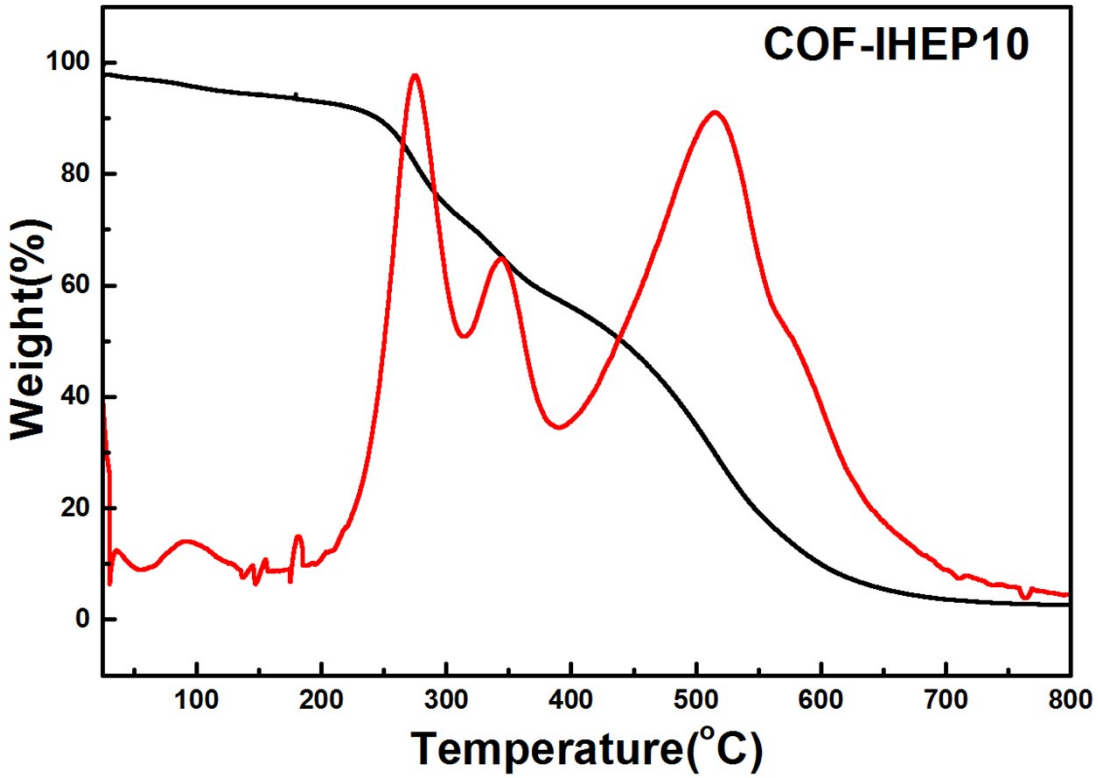

Figure S19. Thermogravimetric Analysis of COF-IHEP10

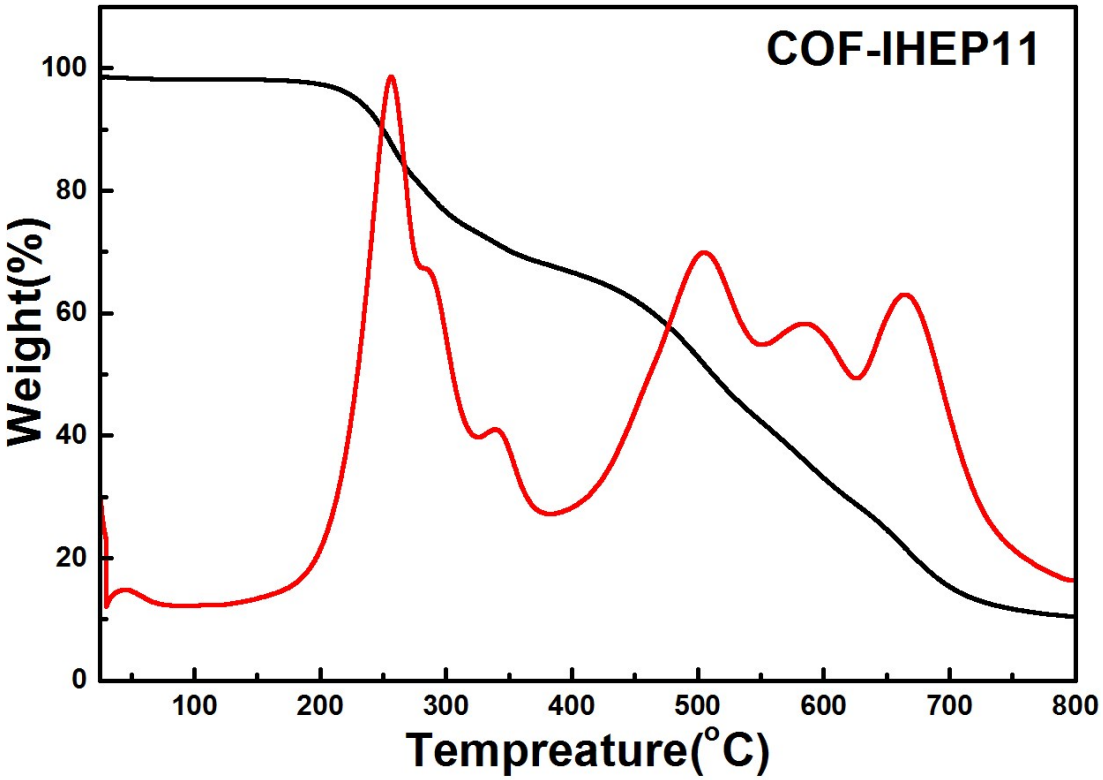

Figure S20. Thermogravimetric Analysis of COF-IHEP11

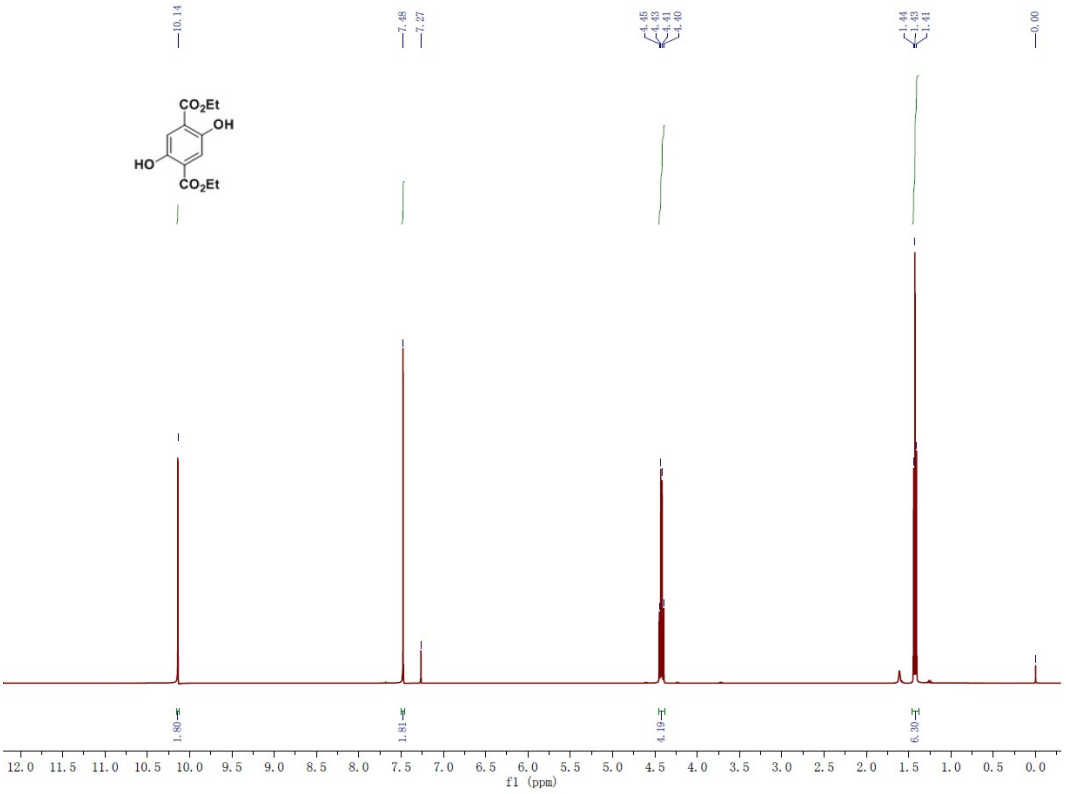

Figure S21. ^{1}H NMR spectra of compound B

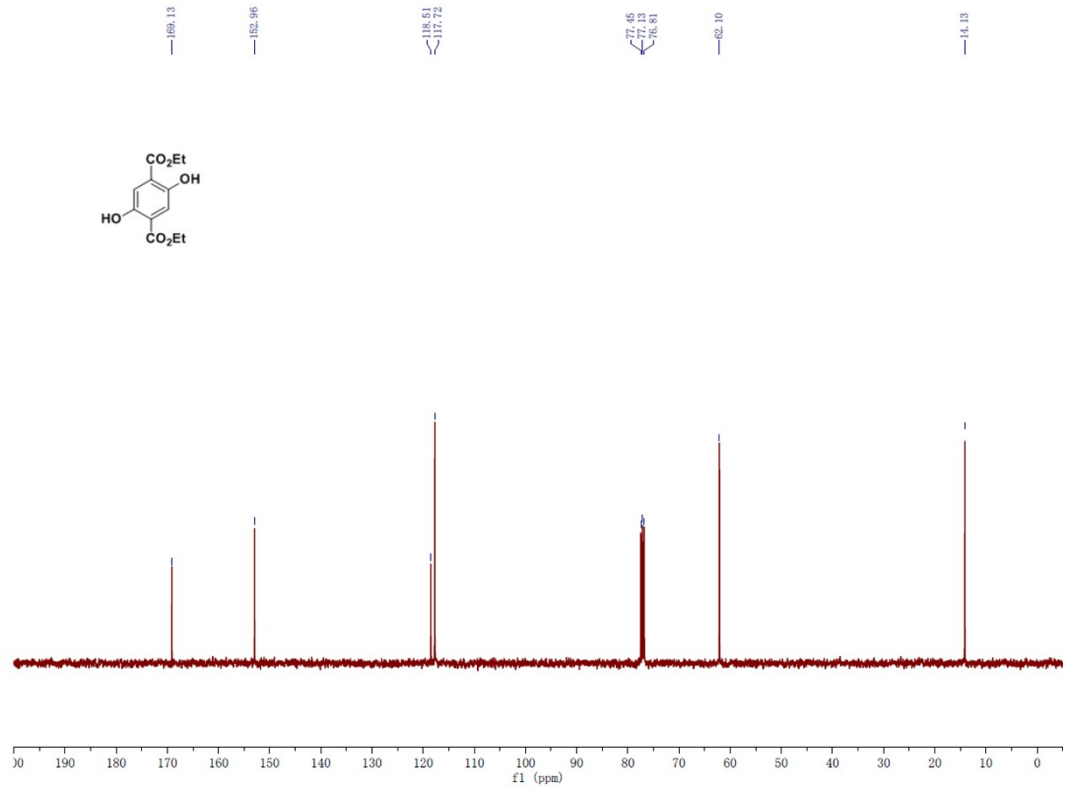

Figure S22. ^{13}C NMR spectra of compound B

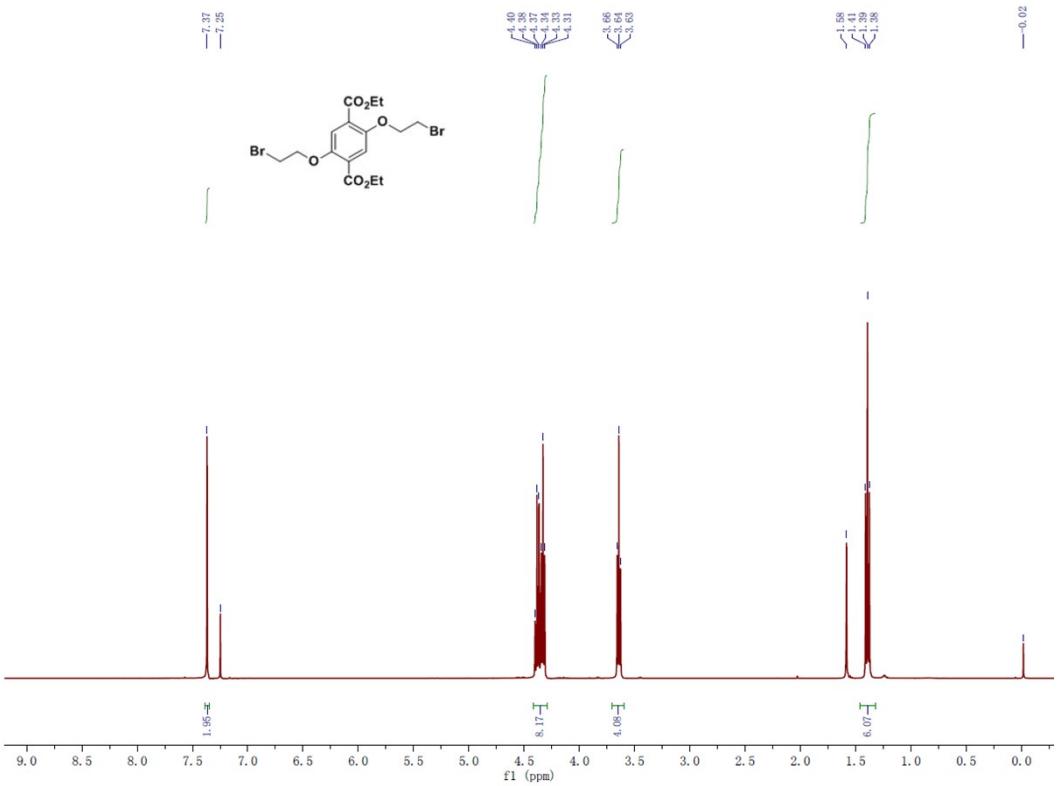

Figure S23. ^{1}H NMR spectra of compound C

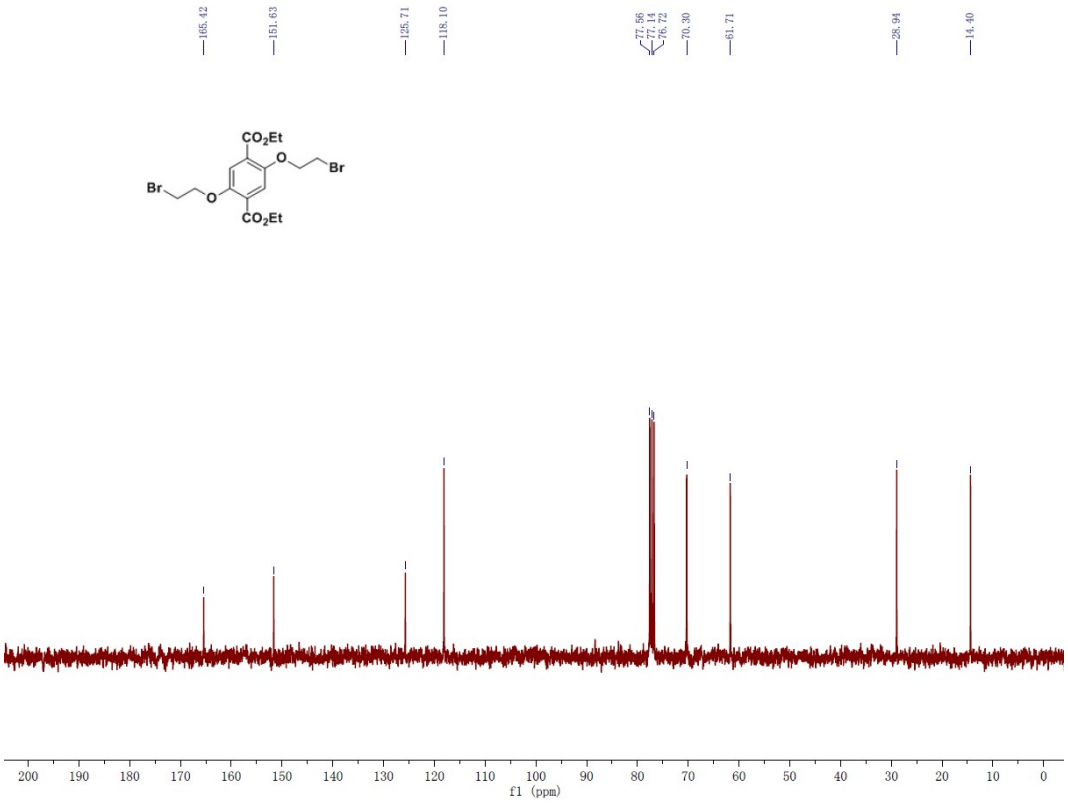

Figure S24. ^{13}C NMR spectra of compound C

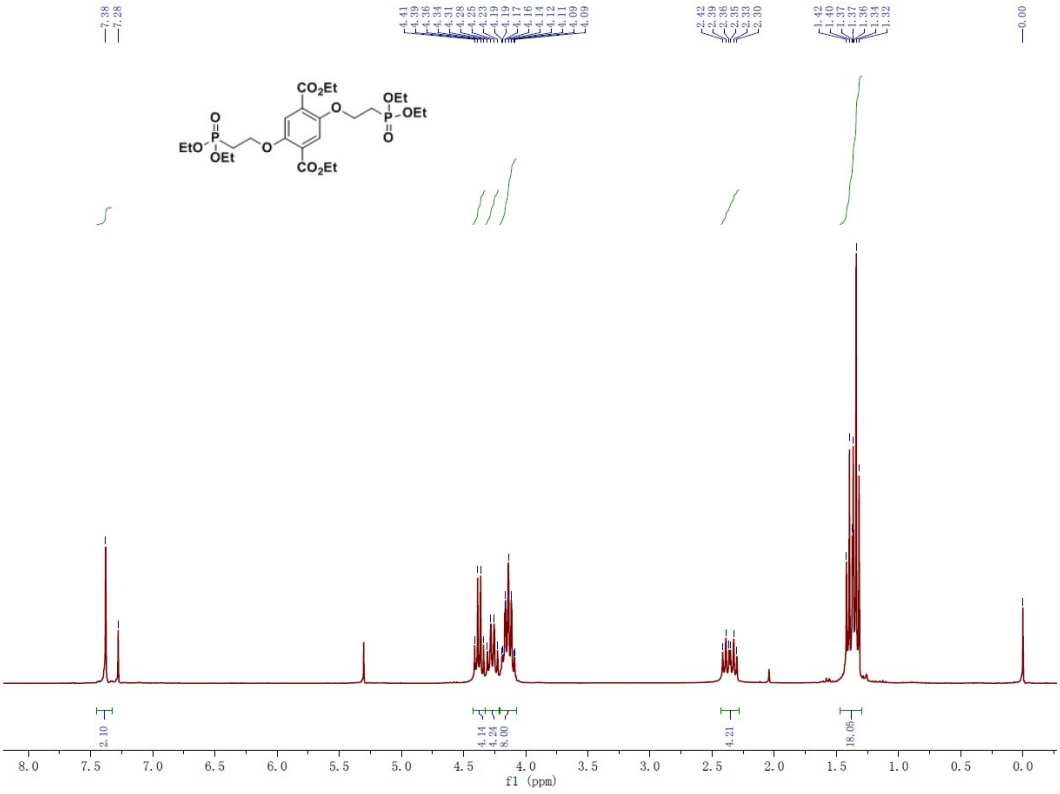

Figure S25. ^{1}H NMR spectra of compound D

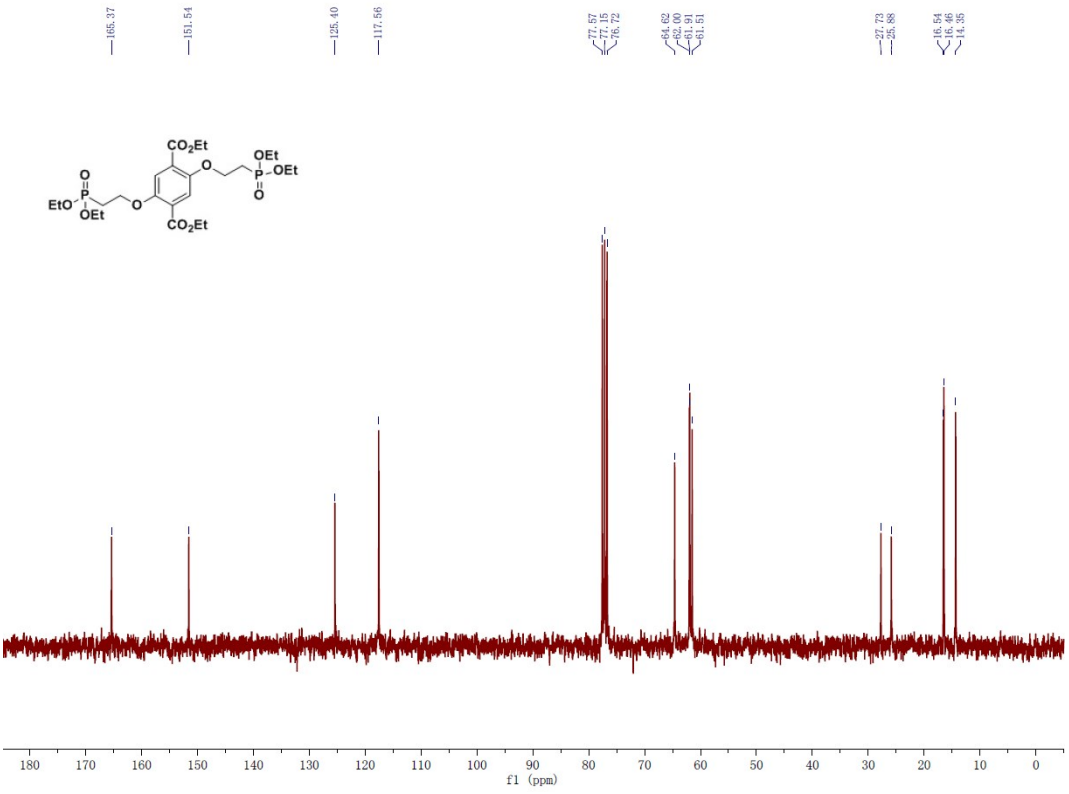

Figure S26. ^{13}C NMR spectra of compound D

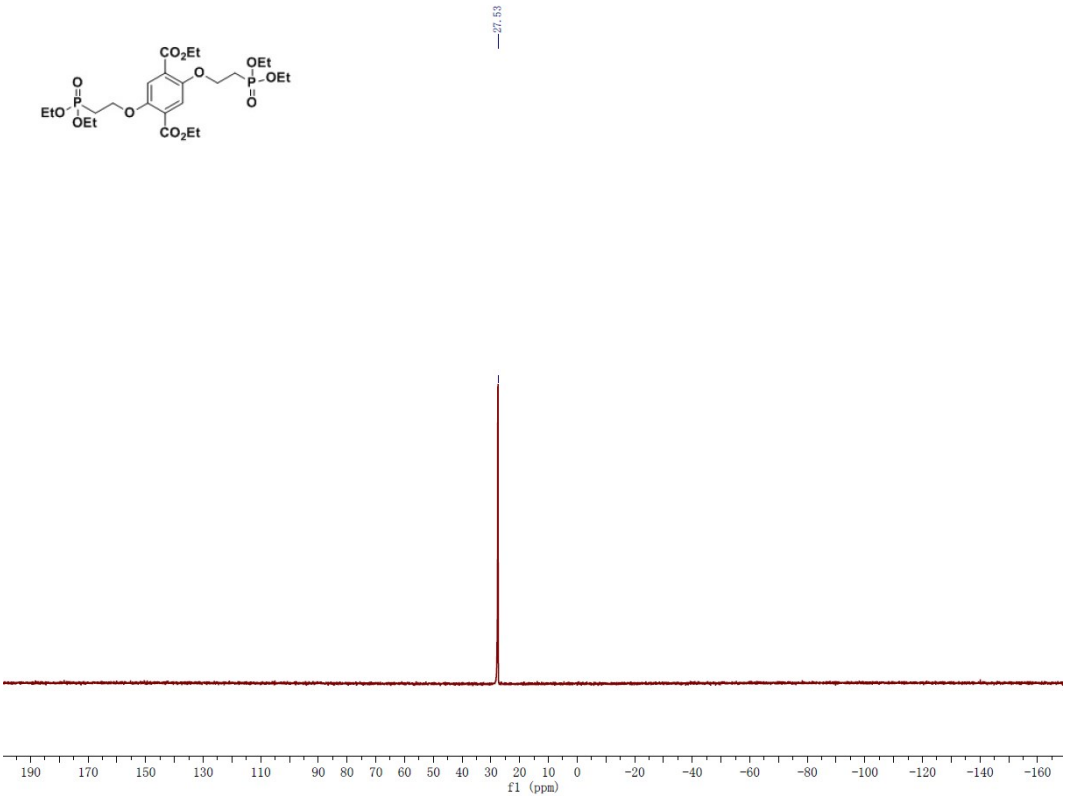

Figure S27. ^{31}P NMR spectra of compound D

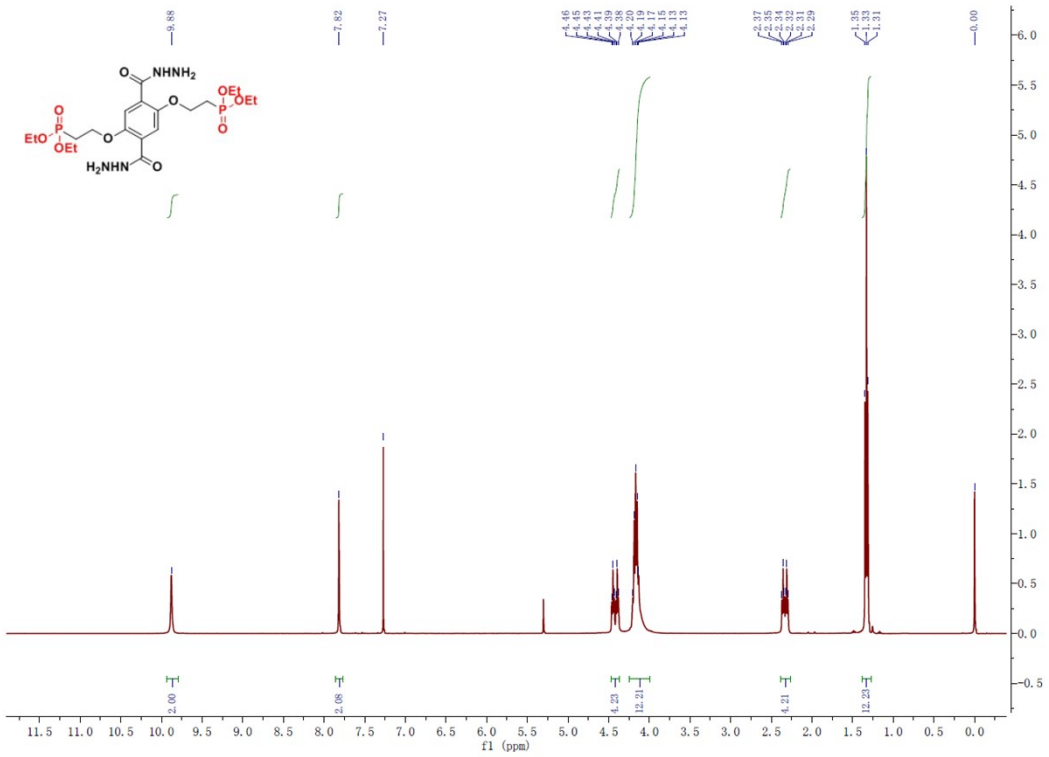

Figure S28. ^{1}H NMR spectra of compound TBBP

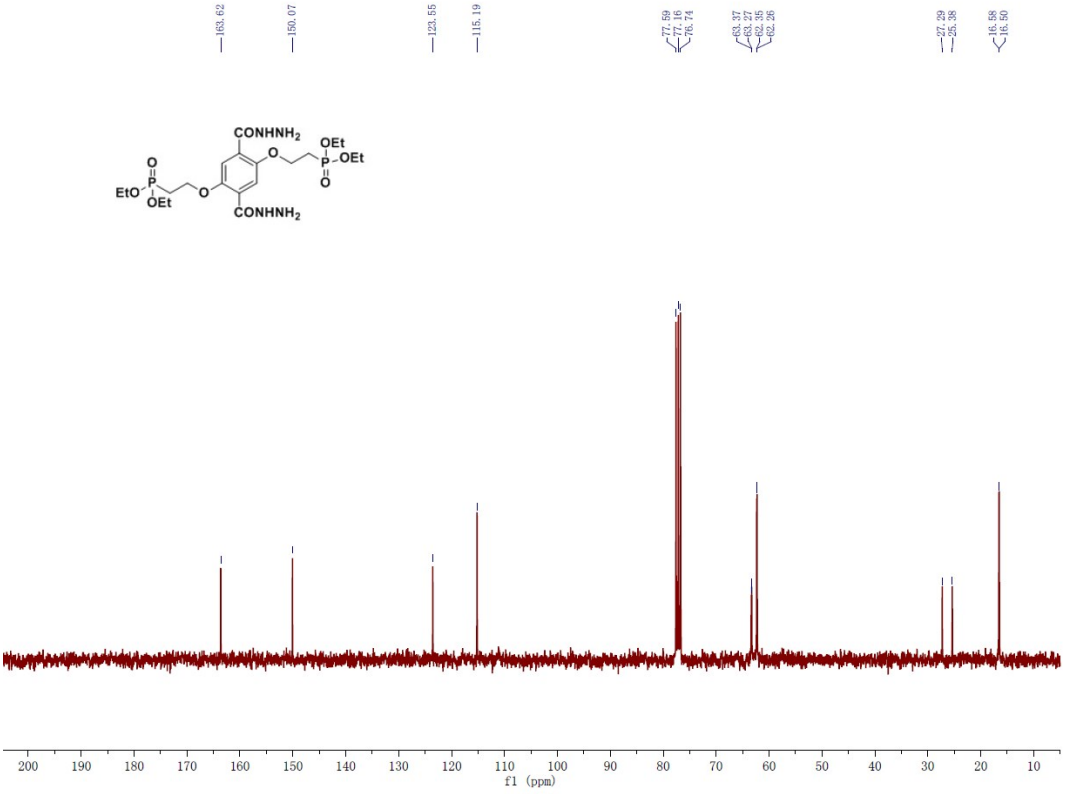

Figure S29. ^{13}C NMR spectra of compound TBBP

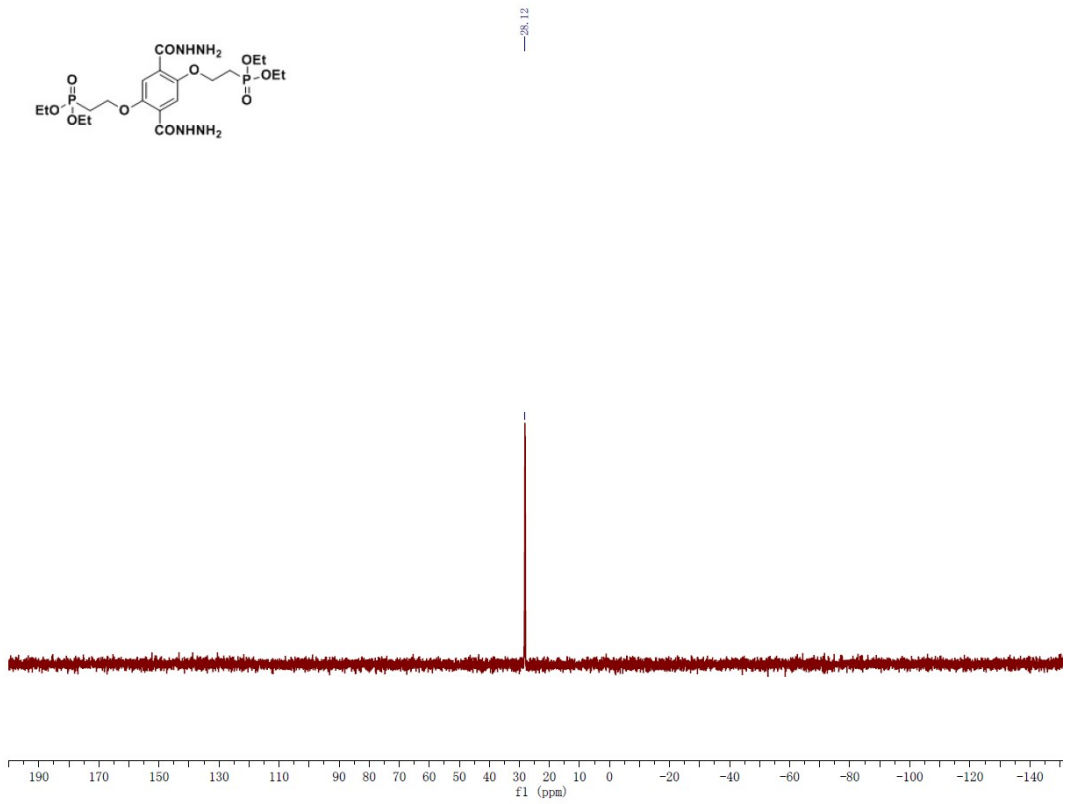

Figure S30. ^{31}P NMR spectra of compound TBBP

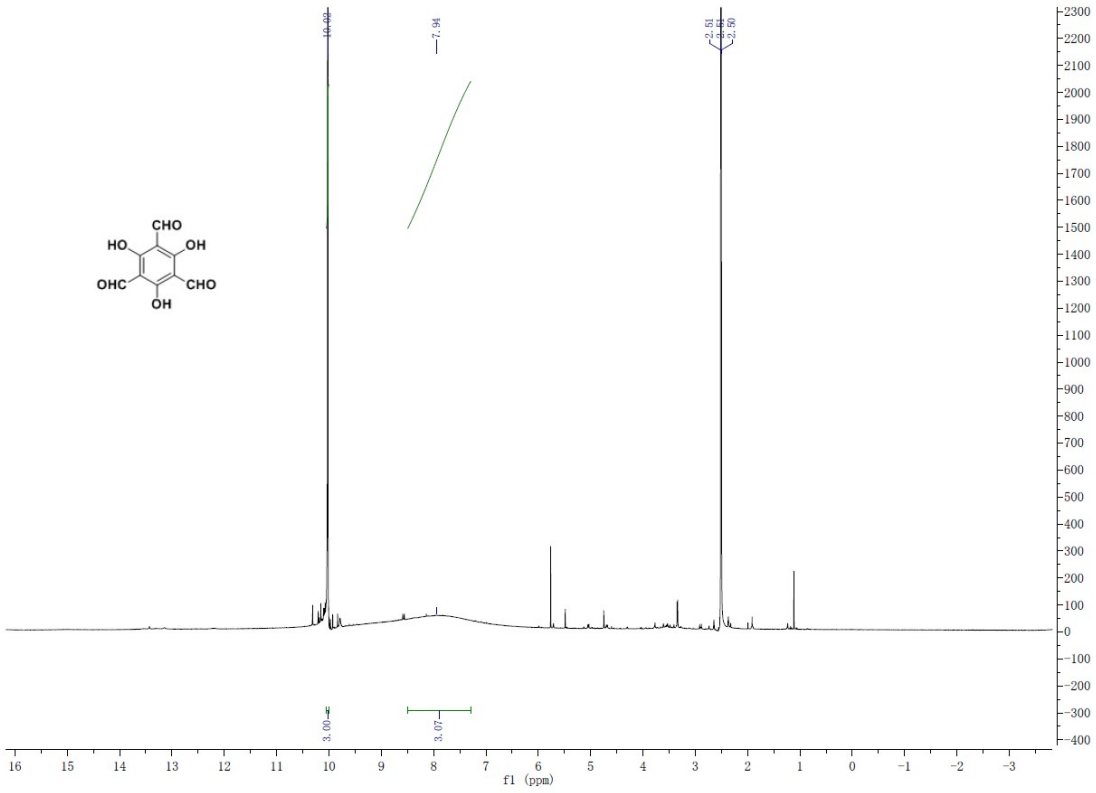

Figure S31. ^{1}H NMR spectra of compound TBTA

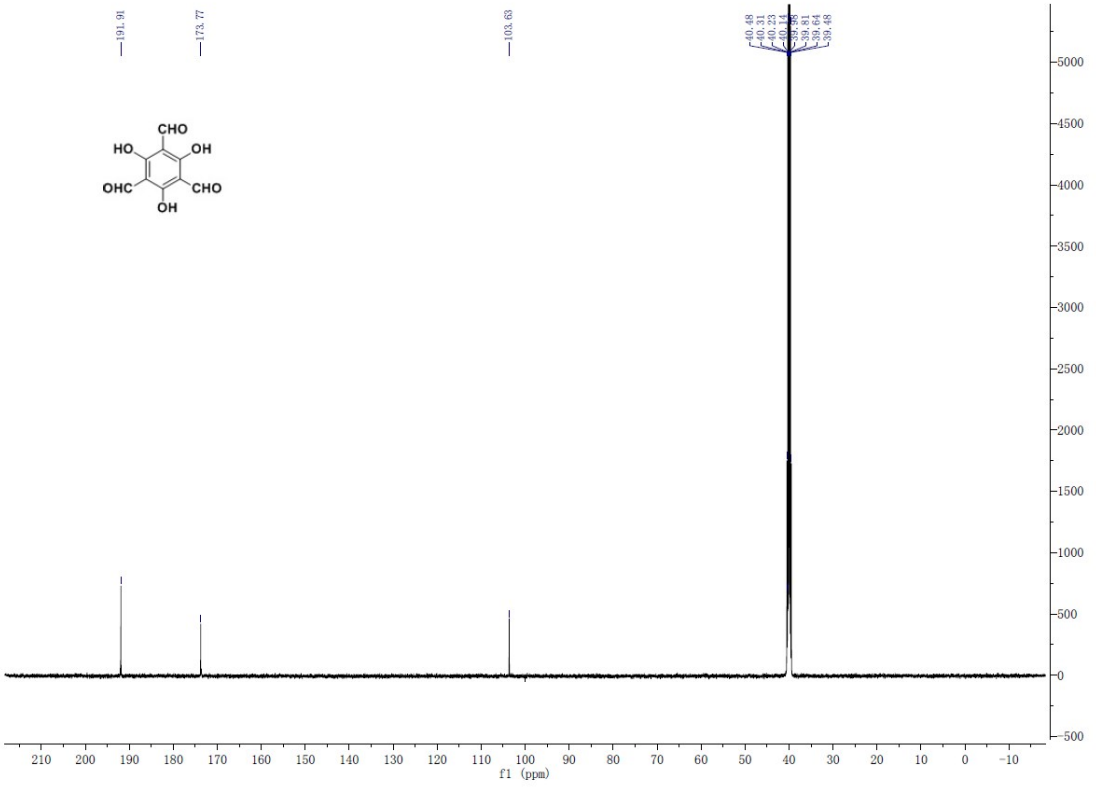

Figure S32. ^{13}C NMR spectra of compound TBTA

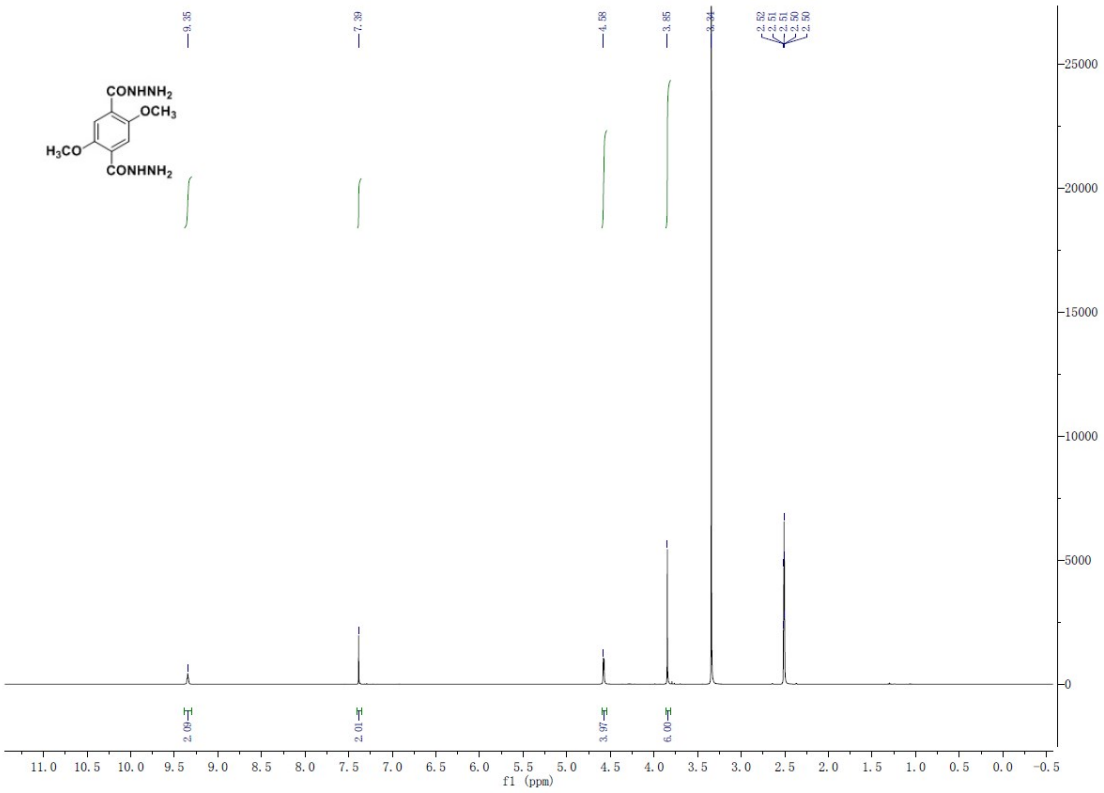

Figure S33. ^{1}H NMR spectra of compound DMPA

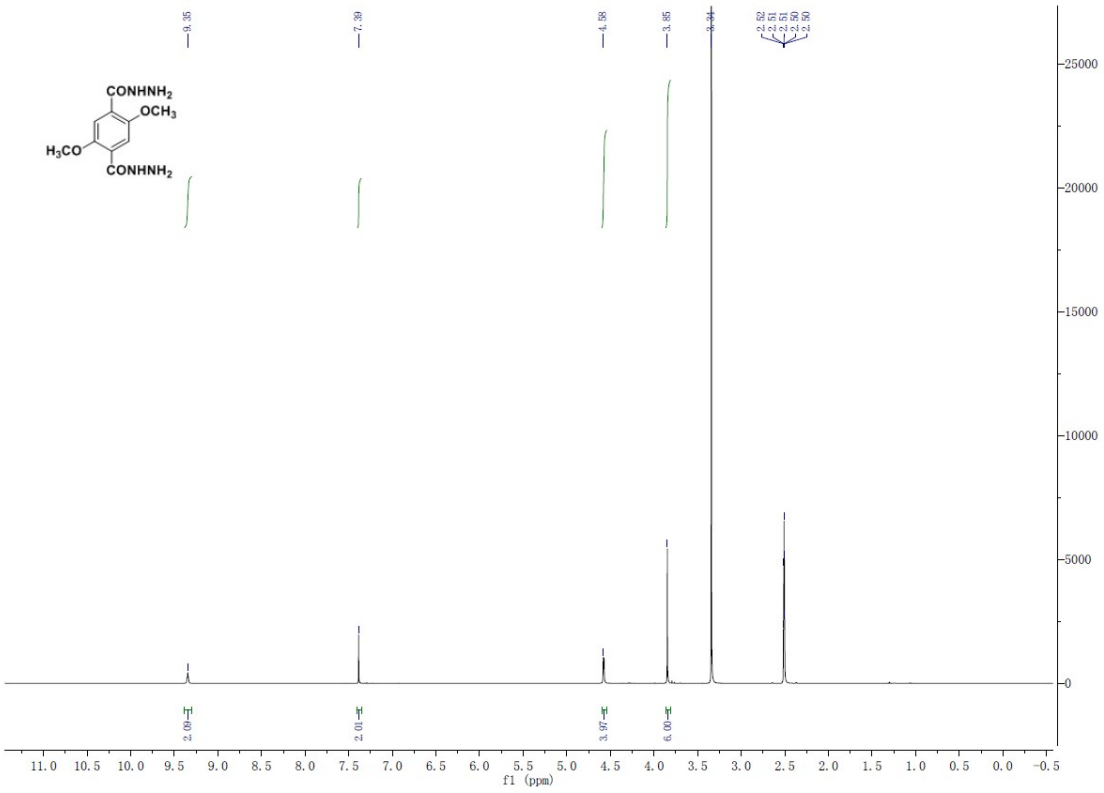

Figure S34. ^{13}C NMR spectra of compound DMPA

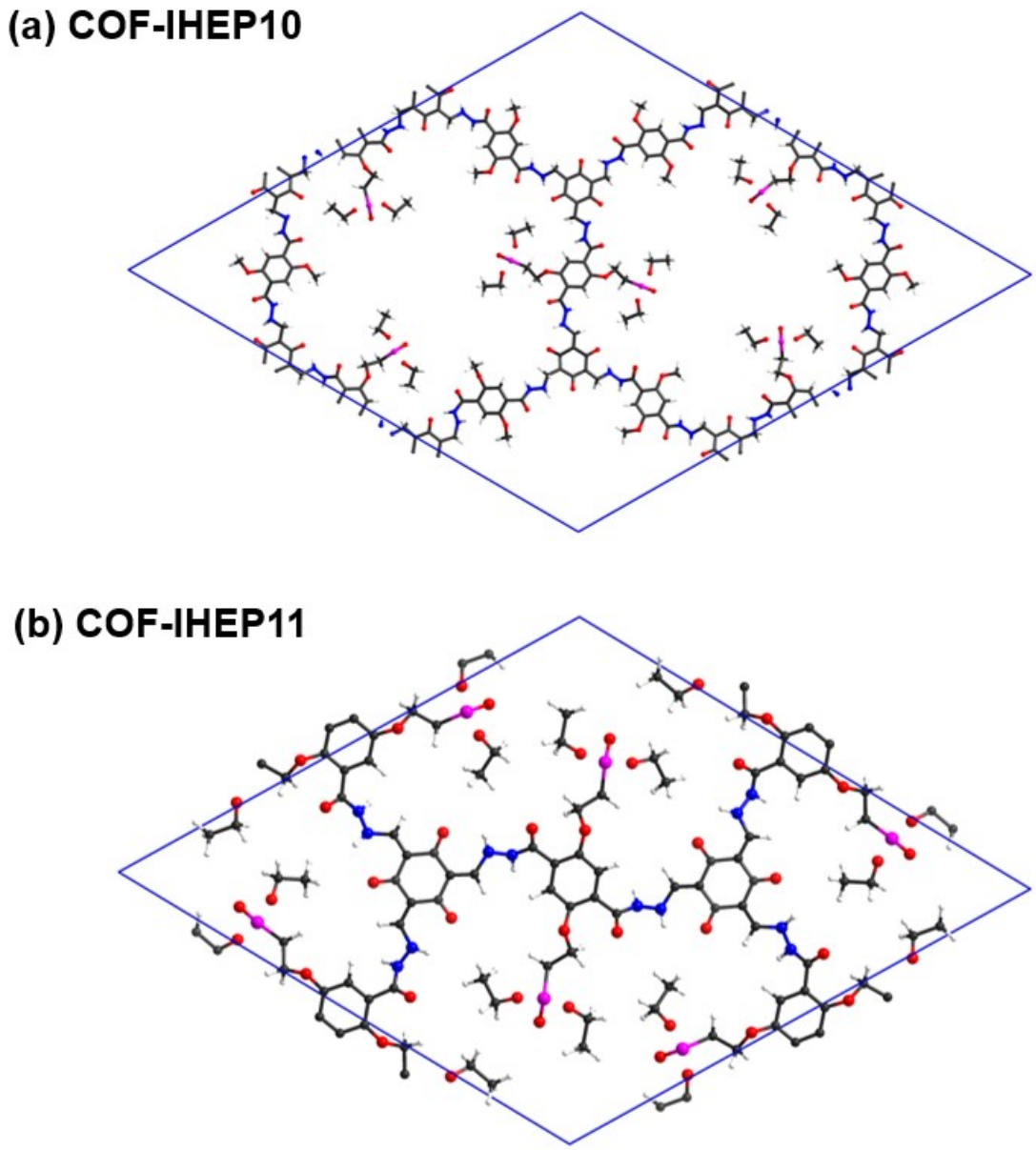

Figure S35. Structure simulation of COF-IHEP10 and COF-IHEP11 in bnn packing mode. C, grey; N, blue; O, red; H, white; P, pink.

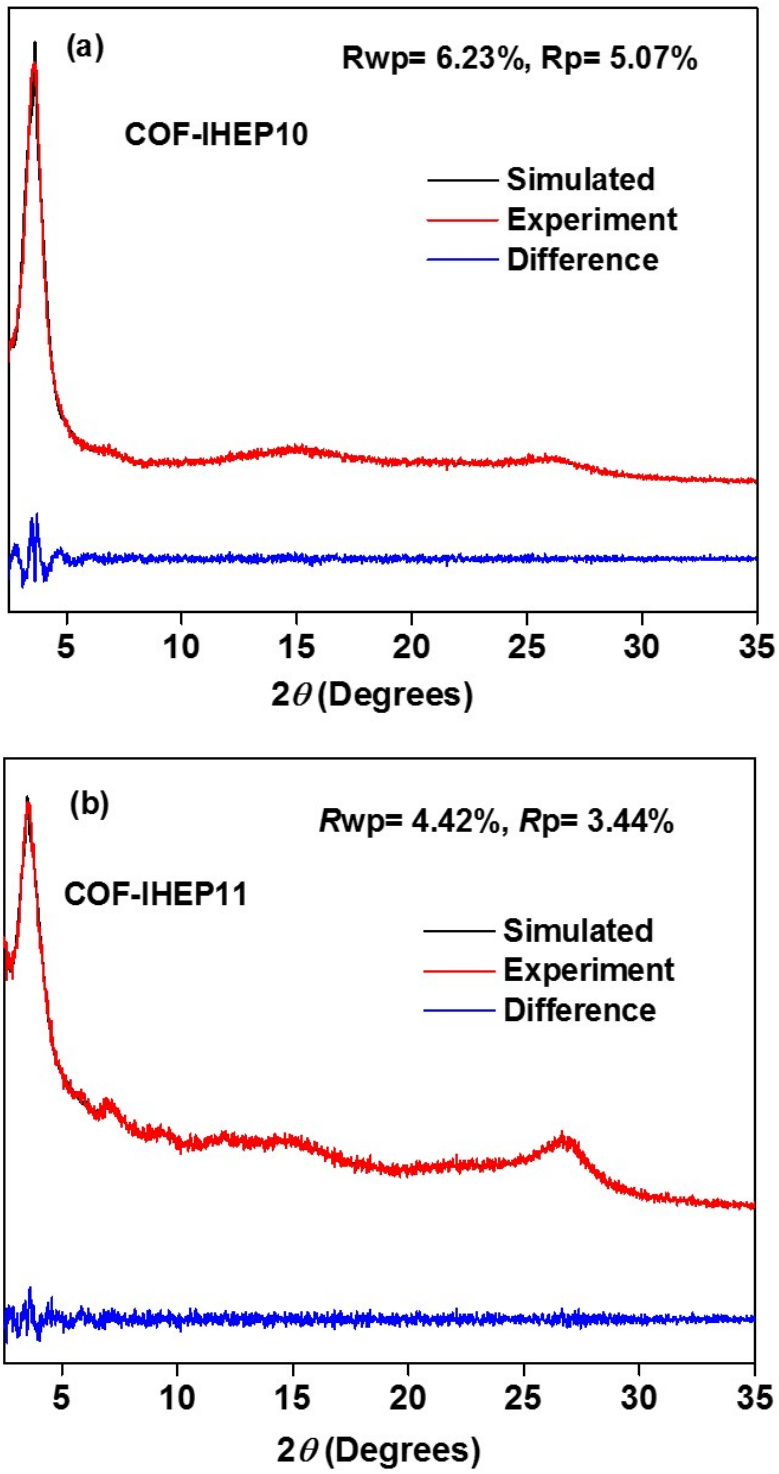

Figure S36. The PXRD profiles from our experiments and Pawly refinement as well as their differences.

Supplementary Tables

Table S1. Fractional atomic coordinates of COF-IHEP11 bnn.

Simulated: hexagonal P6; a=b= 28.826 Å, c= 3.6 Å*			
Atom	*x*/*a*	*y*/*b*	*z*/*c*
H1	0.4816	0.6800	1.1056
H2	0.4529	0.5864	0.5935
O3	0.6058	0.5850	1.1116
H4	0.5783	0.4857	1.0113
C5	0.6379	0.6334	0.8992
C6	0.6910	0.6354	0.7797
P7	0.7563	0.6939	0.9736
O8	0.7849	0.6638	1.2525
O9	0.8051	0.7338	0.7302
O10	0.7443	0.7365	1.2619
C11	0.8188	0.6499	1.0522
C12	0.7881	0.5920	0.9048
C13	0.7450	0.7797	1.0655
C14	0.8026	0.8273	1.0008
C15	0.3925	0.7019	0.1068
C16	0.3575	0.7265	0.0744
C17	0.4461	0.4549	-0.0078
C18	0.4561	0.5082	-0.0172
C19	0.5145	0.6078	-0.0228
C20	0.5092	0.5535	-0.0279
C21	0.3983	0.6185	-0.0044
N22	0.4769	0.6153	-0.2077
N23	0.4559	0.6458	-0.0504
O24	0.5488	0.6443	0.1669
O25	0.5590	0.2687	1.1652
H26	0.7679	0.5625	1.1320
H27	0.8170	0.5822	0.7663
H28	0.7569	0.5871	0.7030
H29	0.8433	0.6794	0.8345
H30	0.8489	0.6506	1.2495
H31	0.7198	0.7655	0.8136
H32	0.7246	0.7957	1.2418
H33	0.8064	0.8658	1.1060
H34	0.8119	0.8332	0.7045
H35	0.8338	0.8206	1.1357
H36	0.6917	0.6319	0.4838
H37	0.6891	0.5978	0.8807
H38	0.6153	0.6359	0.6588

H39	0.6475	0.6691	1.0737
H40	0.8019	0.3769	0.9493

*After refinement: space group P6, a = b = 28.473 Å, *c* = 3.591 Å

Table S2. Adsorption rate constants associated with pseudo first, and second order kinetic models

Models and parameters	COF-JLU4	COF-IHEP10	COF-IHEP11
Pseudo first order kinetic model			
q_e (mg • g^{-1})	38.1	62.5	64.8
k_1 (min^{-1})	1.15× 10^{-2}	1.36× 10^{-2}	1.17× 10^{-2}
R^2	0.9891	0.9813	0.9812
Pseudo second order kinetic model			
q_e *(mg·g^{-1})*	75.2	111.1	120.5
k_2 (g • mg^{-1} • min^{-1})	7.06× 10^{-2}	7.22 × 10^{-2}	7.00 × 10^{-2}
R^2	0.9979	0.9986	0.9976

Table S3. Adsorption rate constants associated with isotherm model parameters

Models and parameters	COF-JLU4	COF-IHEP10	COF-IHEP11
Langmuir			
q_m (mg·g^{-1})	109.9	133.3	147.1
k_L (L·mg^{-1})	0.067	0.142	0.1703
R^2	0.9817	0.9901	0.9904
Freundlich			
k_F *(mg · g^{-1})*	16.65	35.05	46.49
n	2.619	3.618	4.202
R^2	0.9949	0.9884	0.987

References

[1] Mitra, S.; Sasmal, H.-S.; Kundu, T.; Kandambeth, S.; lllath, K.; Diaz, D.-D.; Banerjee, R. *J. Am. Chem. Soc.* **2017**, *139*, 4513-4520.

[2] Zhang, Y.-W.; Shen, X.-C.; Feng, X.; Xia, H.; Mu, Y.; Liu X.-M. *Chem. Commun*. **2016**, *52*, 11088-11091.

[3] Uribe-Romo, F. J; Doonan, C. J.; Furukawa, H.; Oisaki, K.; Yaghi, O. M. *J. Am.*

Chem. Soc. **2011**, *133*, 11478-11481.

[4] Perdew, J. P.; Burke, K.; Ernzerhof, M. *Phys. Rev. Lett.* **1996,** *77*, (18), 3865-3868.

[5] Blöchl, P. E. *Phys. Rev. B* **1994**, *50*, 17953-17979.

[6] Perdew, J. P.; Burke, K.; Ernzerhof, M. *Phys. Rev. Lett*. **1996**, *77*, 3865.

[7] Monkhorst, H. J.; Pack, J. D. *Phys. Rev. B* **1976**, *13*, 5188-5192.